

**Der Effekt von Glykierung und Anästhetika auf die Permeabilität der
Bluthirnschranke in Hinblick auf das mikrobielle Traversal an einem neu
etablierten Zellmodell**

Dissertation zur Erlangung des akademischen Grades
Doktor der Medizin (Dr. med.)

vorgelegt
der Medizinischen Fakultät
der Martin-Luther-Universität Halle-Wittenberg

von Veronika Weber
geboren am
Betreuer*in: Prof. Dr. Rüdiger Horstkorte
Gutachter*innen:
Prof. Dr. Andreas Simm, Halle (Saale)
Prof. Dr. Ottmar Huber, Jena

Datum der Verteidigung: 04.07.2024

Referat

Das Ziel dieser medizinischen Dissertation war die Untersuchung der Einflüsse von nicht-enzymatischer Glykierung, Ascorbinsäure und der Einsatz von Anästhetika auf die Permeabilität der Bluthirnschranke.

Der erste Teil der Arbeit bestand aus der Etablierung eines Zellmodells für die Untersuchung der Permeabilität der Bluthirnschranke. Die immortalisierten „transfected human brain endothelial cells“ (THBMEC) wurden auf Kollagen IV- und Fibronectin-beschichteten Filtern kultiviert. Da der Verlust der Barrierefunktion der Bluthirnschranke mit einigen Pathologien assoziiert wird, wie beispielsweise Sepsis oder Meningitis, wurde der mikrobielle Traversal als Quantifizierung der Durchlässigkeit genutzt. Nach Inkubation mit *Escherichia coli* (*E. coli*), einem der relevanten pathogenen Erreger, wurden Proben aus einer Kammer unter den Filtern entnommen und auf Agarplatten kultiviert. Unbehandelte Zellen dienten als Kontrolle, da sie nahezu keine Bakterien im Modell passieren ließen.

Im zweiten Teil wurde das Modell genutzt, um Einflussfaktoren auf die Permeabilität der Bluthirnschranke in Hinblick auf das mikrobielle Traversal und Alterungsprozesse zu untersuchen. Advanced glycation endproducts (AGE) entstehen bei der nicht-enzymatischen Glykierung und deren Konzentration im Blut korreliert mit erhöhtem Lebensalter und altersassoziierten Krankheiten. Die THBMEC wurden in Methylglyoxal (MGO) inkubiert und im Anschluss der mikrobielle Traversal bestimmt. Dieser war erhöht im Vergleich zu der Kontrolle. Bei Zellen, welche mit Ascorbinsäure vor und nach der Behandlung mit MGO inkubiert wurden, konnte eine Reduktion des mikrobiellen Traversals festgestellt werden. Da ebenso Anästhetika mit der erhöhten Inzidenz von postoperativem Delirium im Alter assoziiert sind und hier ein Zusammenhang mit der erhöhten Permeabilität der Bluthirnschranke vermutet wird, wurde Propofol und das Katecholamin Noradrenalin im Modell getestet. Hier konnte ebenso ein Anstieg des mikrobiellen Traversals beobachtet werden, welcher bei zusätzlicher Behandlung mit MGO weiter anstieg.

Die Ergebnissen ließen darauf schließen, dass AGE und Anästhetika, sowie deren Kombination die Permeabilität der Bluthirnschranke für mikrobielle Pathogene im Modell erhöhen. Gleichzeitig sah man im Modell, dass Ascorbinsäure Effekte der Glykierung rückgängig machen oder diese vorbeugen kann.

Weber, Veronika: Der Effekt von Glykierung und Anästhetika auf die Permeabilität der Bluthirnschranke in Hinblick auf das mikrobielle Traversal an einem neu etablierten Zellmodell, Halle (Saale), Univ., Med. Fak., Diss., 61 Seiten, 2024.

Inhaltsverzeichnis

Referat.....	
Inhaltsverzeichnis.....	
Verzeichnis der Abkürzungen und Symbole.....	
1. Einleitung und Zielstellung.....	1
2. Diskussion.....	7
3. Literaturverzeichnis.....	10
4. Thesen.....	15
Publikationsteil.....	16
Analyzing the Permeability of the Blood-Brain Barrier by Microbial Traversal through Microvascular Endothelial Cells.....	17
Glycation Increases the Risk of Microbial Traversal through an Endothelial Model of the Human Blood-Brain Barrier after Use of Anesthetics.....	37
Erklärungen.....	

Verzeichnis der Abkürzungen und Symbole

Abkürzungen	Bedeutung
AGE	Advanced glycation endproducts (Endprodukt der fortgeschrittenen Glykierung)
AJ	Adherens junctions (<i>Zonula adhaerens</i> /Gürteldesmosom, <i>Fascia adhaerens</i> /Streifendesmosom, <i>Punctum adhaerens</i> /Punkt-desmosom)
BMEC	Brain microvascular endothelial cells (zerebrale mikrovaskuläre Endothelzellen)
CbpA	Curved DNA binding protein A (Gewundenes DNA-Bindungsprotein A)
CD 31	Cluster of differentiation 31 (Cluster der Differenzierung 31)
cm	Zentimeter
<i>E. coli</i>	<i>Escherichia coli</i>
IL-1 β	Interleukin 1 beta
L	Liter
mg	Milligramm
MGO	Methylglyoxal
mM	Millimol
mL	Milliliter
MTT-Assay	3-(4,5-Dimethylthiazol-2-yl)-2,5-diphenyltetrazoliumbromid-Assay (Zellviabilitäts-Assay)
ng	Nanogramm
nM	Nanomol
Opa/-c	Outer membrane adhesin (Adhäsion der Außenmembran)
PAFR	Platelet-activating factor receptor (Rezeptor des Thrombozytenaktivierungsfaktor)
PECAM	Platelet and endothelial cell adhesion molecule (Thrombozyten-Endothelzellen-Adhäsionsmolekül)
PilQ	Pilin-like protein Q (Pilin-ähnliches Protein Q)

pIgR	Polymeric immunoglobulin receptor (Immunoglobulinpolymer-Rezeptor)
POD	Postoperatives Delirium
RAGE	Receptor of advanced glycation endproducts (Rezeptor der Endprodukte fortgeschrittener Glykierung)
ROS	Reactive oxygen species (Reaktive Sauerstoffspezies)
TEER	Transendothelial electrical resistance (transendothelialer elektrischer Widerstand)
TGF- β	Transforming growth factor beta (transformierender Wachstumsfaktor beta)
TNF- α	Tumor necrosis factor alpha (Tumornekrosefaktor alpha)
THBMEC	Transfected human brain endothelial cells (transfizierte humane zerebrale Endothelzellen)
TJ	Tight junctions (<i>Zonula occludens</i> , Schlussleiste)
VE-Cadherin	Vascular endothelial cadherin (vaskuläres endotheliales Cadherin)
VEGF	Vascular endothelial growth factor (vaskulärer endothelialer Wachstumsfaktor)
Ω	Ohm
μg	Mikrogramm

1. Einleitung und Zielstellung

Die Bluthirnschranke bildet eine Barriere im menschlichen Körper, um das Gehirn vom Blut zu separieren. Dies schützt das Gehirn vor Toxinen, Mikroben und Fluktuationen im Plasma und reguliert Stoffwechselfvorgänge. Sie besteht aus drei verschiedenen Zelltypen, doch die Undurchlässigkeit wird vor allem durch die hohe Anzahl der Tight-Junctions (TJ) und Adherens-Junctions (AJ) (1) der mikrovaskulären Endothelzellen sowie die Kollagen IV- und Fibronektin-reiche Basalmembran (2,3) gewährleistet. Kleinere lipophile Moleküle können per Diffusion passieren, während größere und hydrophile Moleküle nur über ein spezialisiertes Transportsystem passieren (4,5). Dies ist messbar als transendothelialer elektrischer Widerstand (TEER), welcher an einer intakten Bluthirnschranke 1500-2000 $\Omega \cdot \text{cm}^2$ beträgt (6).

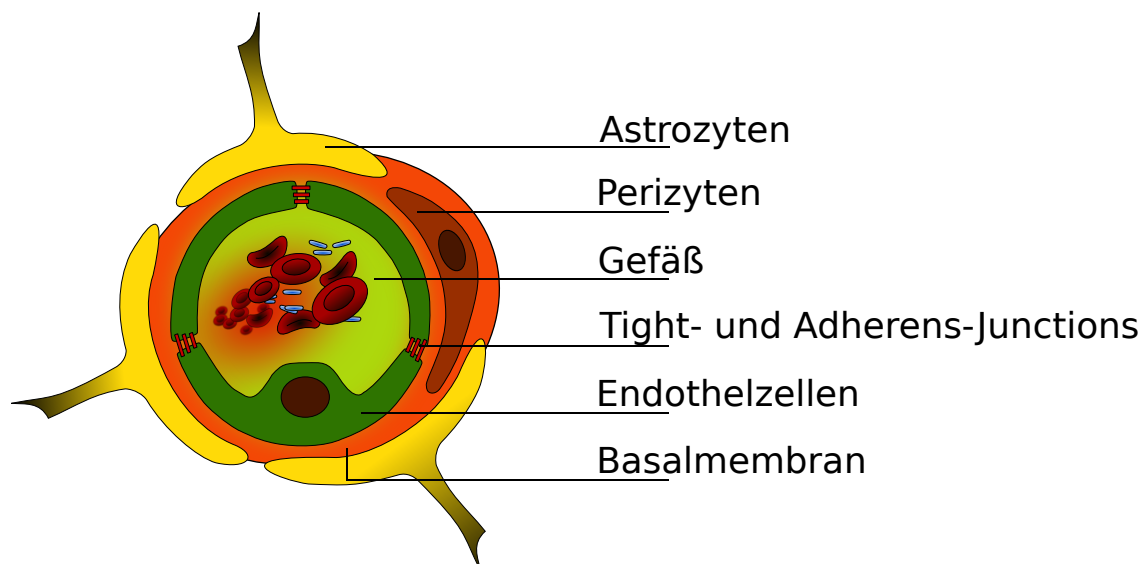


Abbildung 1: Aufbau der Bluthirnschranke - modifiziert nach Weber et. al.

Die Bluthirnschranke ist aus drei verschiedenen Zelltypen aufgebaut. Die direkte Begrenzung des Blutes bilden die mikrovaskulären Endothelzellen. Diese können durch zahlreiche Tight-Junctions und Adherens-Junctions und fehlende Fenestrierung eine Barriere gegen größere und hydrophile Moleküle sowie Pathogene aufbauen. Daneben sind Perizyten wichtig für die Stabilität der Gefäßwand und spielen eine Rolle in der Entwicklung der Bluthirnschranke wie auch die Astrozyten. Deren Endfüße bilden eine Schicht um das Gefäß und unterstützen die Bildung von Tight-Junctions. Alle Komponenten der Bluthirnschranke sind wichtig für deren Funktionalität.

Viele Pathologien wurden mit einem Zusammenbruch der Bluthirnschranke in Verbindung gebracht. So zum Beispiel das postoperative Delirium (POD), welches gekennzeichnet ist durch eine Störung der Aufmerksamkeit und des Bewusstseins mit einem fluktuierenden Verlauf 5 Tage nach einer Operation (7). Die fehlende Barriere

der Bluthirnschranke scheint zu einer Exazerbation der systemischen Inflammation und Erhöhung der Konzentration von Chemokinen im Gehirn zu führen (8,9). In einer Studie zum POD nach einer Operation bei älteren Patienten konnte eine unabhängige Assoziation mit postoperativer Sepsis (10) und präoperativen Infektionen (11,12) festgestellt werden. Eine weitere intensiv erforschte Pathologie ist die septische Enzephalopathie. Diese entsteht im Rahmen einer Sepsis und ist über eine veränderte Gehirnfunktion durch die Anwesenheit von Mikroorganismen oder deren Toxine im Blut definiert (13). Da sie schon früh während einer Sepsis auftreten kann, sind am ehesten proinflammatorische Mediatoren ätiologisch für den Endothelschaden im Gehirn. In septischen Tiermodellen wurde eine erhöhte zerebrale Aufnahme von neutralen Aminosäuren gemessen, ebenso eine erhöhte extravasale Konzentration von Meerrettichperoxidase im Vergleich zu gesunden Tieren (14,15), was eine erhöhte Permeabilität der Bluthirnschranke vermuten lässt. Um den mikrobiellen Traversal direkt in Bezug zu der Permeabilität der Bluthirnschranke zu untersuchen, etablierte ich ein neues Modell. Da für die Undurchlässigkeit der Bluthirnschranke vor allem die mikrovaskulären Endothelzellen und das Basalmembran relevant sind, kultivierte ich immortalisierte „transfected human brain endothelial cells“ (THBMEC) (16) auf Fibronectin- und Kollagen IV-beschichteten Filtern. Die Dauer der Kultivierung stützte sich auf Daten aus Voruntersuchungen, in denen die niedrigste Permeabilität zwischen Tag 13 und 15 gemessen wurde (17). *Escherichia coli* (*E. coli*) ist ein möglicher Erreger bei Meningitis (18), einer Entzündung der Hirnhäute, welche zu einem zerebralen Ödem und einer komplexen Inflammation führt. Als mögliche Eintrittspforte wird das mikrovaskuläre Gefäßsystem diskutiert (19). Als ebenfalls gut etabliertes Bakterium im Labor verwendete ich dieses im Modell. Mittels Bestimmung der optischen Dichte wurde die Anzahl der Bakterien standardisiert, um diese dann in die Kammern oberhalb der Filter zu geben und nach der Inkubationszeit aus den Kammern unterhalb der Filter Proben zu entnehmen. Diese wurden auf Agarplatten ausgestrichen und die gebildeten Kolonien gezählt. Ich bestimmte ebenfalls den TEER für dieses Modell mit einem Wert von $70 \Omega \cdot \text{cm}^2$. Dies ist vergleichbar mit Werten anderer etablierter Modelle (20). Ich führte keine regelhafte Bestimmung durch, da die unbehandelten Zellen keine Bakterien durchließen und mir dies als Kontrolle diente.

Da es sich bei den THBMEC um eine neue Zellreihe in unserem Labor handelte, wollte ich diese bezüglich der Proteinexpression und Reaktion auf Zellsignale näher charakterisieren. Dabei fokussierte ich mich auf die wichtigsten Proteine für die niedrige Permeabilität der Bluthirnschranke sowie auf proinflammatorische Signale. Die

mikrovaskulären Endothelzellen der Bluthirnschranke unterscheiden sich von anderen Endothelzellen vor allem durch die hohe Anzahl an TJ und AJ (1), sowie ein kontinuierliches Basalmembran (2,3). Im Verlauf der Kultivierung der THBMEC legte ich besonderes Augenmerk auf die Expression der interzellulären Verbindungen bis zu dem Zeitpunkt, an welchem die Zellen eine undurchlässige Barriere gegen die Bakterien gebildet hatten. Occludin ist ein Markerprotein der TJ (21,22), VE-Cadherin ist ein Transmembranprotein, welches die AJ bildet (23). Beide wurden mittels Antikörper im Westernblot detektiert und durch eine Software ausgewertet. Zwischen Tag 2 und Tag 16 der Kultivierung auf den Filtern ergab sich ein signifikanter Anstieg der beiden Proteine. Ein weiteres Protein für Zelladhärenz und Zellsignalwege ist Integrin-1-beta. Hier konnte ich keinen Anstieg über den Zeitraum feststellen. Ebenso interessierte mich die immunologische Antwort der THBMEC auf proinflammatorische Signale. Hierfür behandelte ich die Zellen mit Interleukin 1-beta (IL-1 β) und Tumornekrosefaktor alpha (TNF- α) (24). Als Marker bestimmte ich mittels Antikörper im Westernblot in den behandelten Zellen das Thrombozyten-Endothelzellen-Adhäsionsmolekül (PECAM). Dieses Protein ist als Cluster der Differenzierung 31 (CD 31) bekannt und reguliert vor allem die Leukozyten-Transmigration. Hier ergab sich ein signifikanter Anstieg nach Behandlung der Zellen.

Das Verständnis von Alterungsprozessen auf molekularer Ebene wird immer wichtiger bei einer alternden Gesellschaft. Das Altern ist komplex und multifaktoriell mit endogenen, genetischen und umweltbezogenen Aspekten (25). Einer dieser molekularen Aspekte ist die Entstehung von Advanced glycation endproducts (AGE) über die nicht-enzymatische Glykierung. Diese posttranslationalen Modifikationen von zellulären Proteinen verändern deren Funktion und führen zum Teil zu einem kompletten Verlust dieser. So zeigte sich bei Glykierung von Mitochondrienproteinen und antioxidativen Enzymen wie Glutathionreduktase oder Glutathionperoxidase in Ratten ein Anstieg des oxidativen Stresses durch Veränderungen der Proteinfunktion (26,27). Ebenso ergab sich bei steigender AGE-Konzentration eine Abnahme der Funktion der Glyceraldehyd-3-Phosphat Dehydrogenase (28). Die nicht-enzymatische Glykierung findet als Kondensationsreaktion zwischen den Carbonylgruppen von Kohlenhydraten oder deren Metaboliten mit freien Aminogruppen statt. Das gebildete labile Zwischenprodukt, die Schiffsche Base, wird über die Säure-Base-Katalysation rearrangiert zu einem stabileren Ketoamin, das Amadoriprodukt. Ein kleiner Teil dieser Amadoriprodukte unterliegt weiteren irreversiblen Reaktionen, sodass durch Proteinaddukte und -quervernetzungen AGE gebildet werden (29,30).

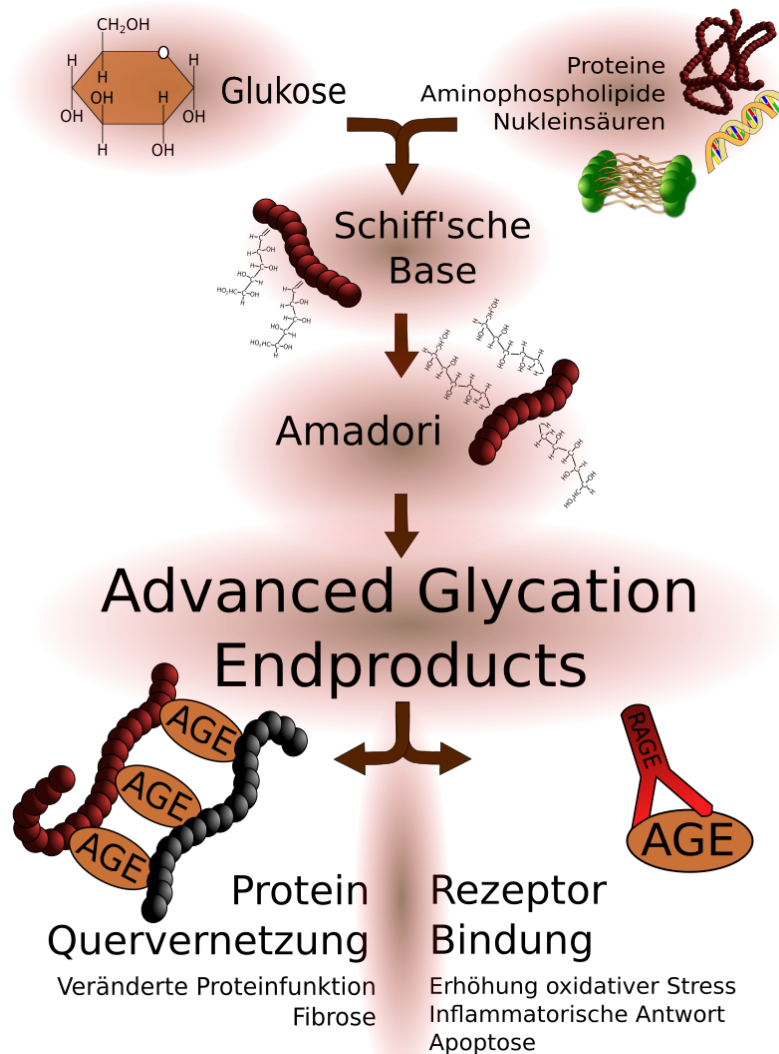


Abbildung 2: Advanced glycation endproducts

Die Carbonylgruppe der Glucose und die freie Aminogruppe von Proteinen, Nukleinsäuren oder Aminophospholipiden führt über eine Kondensationsreaktion zu einem instabilen Zwischenprodukt, der Schiffschen Base. Diese rearrangiert sich zum Teil zum stabileren Amadoriprodukt. Und von diesen wird ein Teil durch irreversible Reaktionen zu den Advanced glycation endproducts. Diese können über Proteinquervernetzungen die Proteinfunktionen beeinträchtigen. Gleichzeitig binden sie an ihren Rezeptor (RAGE) und führen so zu vorzeitiger Apoptose, vermehrtem oxidativen Stress oder inflammatorischen Reaktionen im Gewebe.

Deren Konzentration steigt physiologisch mit steigendem Alter, jedoch korreliert sie auch mit altersassoziierten Erkrankungen wie Diabetes mellitus (31). Hier konnte ein zweifach erhöhtes Risiko für Meningitis und Enzephalitis durch Hyperglykämie festgestellt werden (32–34). Dies hat verschiedene Ursachen wie beispielsweise eine Immunsuppression. In Untersuchungen konnte zusätzlich gezeigt werden, dass AGE zu einer erhöhten Permeabilität der Bluthirnschranke durch Reduzierung der Claudin

5-, Zonula occludens-1- und Occludinexpression mit Einfluss auf die Zellverbindungen und autokrinen Signalwege (35) führen. Ebenso werden proinflammatorische Signale hochreguliert wie die transformierenden Wachstumsfaktoren beta (TGF- β) und die vaskulären endothelialen Wachstumsfaktoren (VEGF) (36,37). Außerdem wurde Diabetes als unabhängiger Risikofaktor für das POD identifiziert (38). Deshalb interessierte mich der Einfluss der AGE auf die Bluthirnschranke im Modell. Fragmentationen der Amadoriprodukte führen zu der Bildung von Methylglyoxal (MGO), welches ebenfalls ein Nebenprodukt der Glykolyse ist. Es ist ein hochreaktives Dicarbonyl und führt zu der Bildung von verschiedenen AGE. Ich behandelte die THBMEC mit verschiedenen Konzentrationen von MGO und detektierte mit Antikörpern die Bildung von AGE im Westernblot. Bei 0,15 mM war die niedrigste Konzentration, bei der AGE nachgewiesen werden konnten. In einem Zellviabilitäts-Assay (MTT-Assay) konnte keine Zytotoxizität dieser MGO-Konzentration festgestellt werden, sodass ich diese Konzentration für die weiteren Experimente verwendete. Im Modell behandelte ich die THBMEC nach 14 Tagen Kultivierung auf den Filtern mit MGO 0,15 mM für 1 Stunde. Danach bestimmte ich den mikrobiellen Traversal. Hier konnte ein signifikanter Anstieg zu den unbehandelten Zellen beobachtet werden.

Ascorbinsäure, auch bekannt als Vitamin C, ist ein Antioxidans mit positiven Effekten auf die Permeabilität der glykierten Bluthirnschranke (39). Gleichzeitig hat es selbst das Potenzial zur Glykierung. Die THBMEC wurden für 4 Stunden mit 0,1 mM Ascorbinsäure behandelt. Sowohl bei der Behandlung vor der Glykierung mit MGO, als auch nach der Glykierung mit MGO ergab sich eine signifikante Reduktion des mikrobiellen Traversal.

Zum besseren Verständnis des POD durch eine erhöhte Permeabilität der Bluthirnschranke, wollte ich Anästhetika im Modell testen. Propofol ist eines der geläufigen Anästhetika, welches zellulären Stress induziert und den Zusammenbruch der Bluthirnschranke unterstützt (40,41). Weitere Studien zeigten einen neuroprotektiven Effekt durch antioxidative und anti-inflammatorische Eigenschaften von Propofol (42,43) und eine Verringerung der POD-Inzidenz im Vergleich zu anderen Anästhetika (44). Noradrenalin ist ein oft genutztes Katecholamin in einer Anästhesie. Ich suchte in der Literatur nach möglichen Konzentrationen von Propofol und Noradrenalin während einer Anästhesie im menschlichen Blut (45–47). Die Dauer der Behandlung richtete sich nach der durchschnittlichen Operationsdauer von 3 Stunden für Propofol, sowie der überwiegenden Anwendung von Noradrenalin als Bolusinjektion

für 1 Stunde. Für die gefundenen Konzentrationen von 3 µg/mL Propofol für 3 Stunden sowie 1 ng/mL Noradrenalin für 1 Stunde konnten im MTT-Assay keine Zytotoxizität festgestellt werden. Im Modell ergab sich ein signifikanter Anstieg des mikrobiellen Traversal nach Propofol- und Noradrenalinbehandlung im Vergleich zu unbehandelten Zellen. Um die Effekte der AGE während einer Operation näher zu untersuchen, wurden mit MGO 0,15 mM glykierte Zellen zusätzlich mit Propofol und Noradrenalin behandelt. Diese doppelt behandelten Zellen zeigten im Modell einen signifikanten Anstieg des mikrobiellen Traversals im Vergleich zu unbehandelten Zellen und ausschließlich mit Propofol oder Noradrenalin behandelten THBMEC.

2. Diskussion

Das bisher unvollständige Verständnis der Pathogenese des mikrobiellen Traversal an der Bluthirnschranke erfordert weitere Grundlagenforschung und hier bildet das neu etablierte Zellmodell eine wichtige Ergänzung. Dieses Modell bietet den Vorteil eines unkomplizierten Aufbaus mit Equipment, welches in den meisten Laboren in diesem Forschungsfeld existiert. Des weiteren gibt es die Möglichkeit die verwendeten Stoffe zur Behandlung der Zellen und Erreger zu erweitern, um deren Einfluss auf die Bluthirnschranke zu erforschen. Messungen des TEER oder die Markierung mit Tracern können ohne Probleme im Modell ergänzt werden. Ebenso wäre eine Automatisierung mit Filtern einer 96-well Platte möglich. Dies könnte ein Hochdurchsatz-Medikamentenscreening ermöglichen mit dem Ziel Einflüsse der Medikamente auf die Bluthirnschranke zu untersuchen und ebenso neue Therapien zu entwickeln.

Die Einschränkungen eines Modells sind vor allem die Vereinfachung der hochkomplexen Vorgänge, so auch die multifaktoriellen Abläufe in den humanen mikrovaskulären Endothelzellen des Gehirns (BMEC) in diesem Zell-Modell. Einige erfolgreiche Isolationen der BMEC aus verschiedenen Spezies führten zu einer veränderten Proteinexpression (48,49). Meine verwendeten Zellen wurden in sehr frühen Passagen transfiziert, sodass die spezifischen Eigenschaften der BMEC erhalten blieben (16). Um der physiologischen Bluthirnschranke noch näher zu kommen ist eine Erweiterung um Astrozyten und Perizyten notwendig, da zwischen den Zelltypen eine enge Interaktion und Regulation herrscht. Astrozyten induzieren die Bildung von TJ und beeinflussen die Reifung der Bluthirnschranke mittels verschiedener Faktoren (50). Perizyten spielen eine wichtige Rolle in der Angiogenese und verhindern die Apoptose der BMEC (51).

Escherichia coli ist ein gut erforschter pathogener Keim mit einer hohen Inzidenz für Meningitis. Mittels Pili bindet dieses Bakterium an die BMEC, aktiviert die Inflammation und verringert die Anzahl der TJ, um so die Bluthirnschranke zu durchqueren (52). Genaue Wege sind hier noch nicht vollständig verstanden. Ich verwendete im Modell eine Ampicillin-Resistenz, um das Wachstum anderer Bakterien vorzubeugen. In weiterführenden Untersuchungen sollten verschiedene Bakterien untersucht werden, welche ebenfalls Meningitis auslösen können und andere Mechanismen verwenden wie *Streptococcus pneumoniae*. Hier werden verschiedene Rezeptoren wie PECAM-1, Immunoglobulinpolymer-Rezeptor (pIgR) sowie Rezeptor des Thrombozytenaktivierungsfaktor (PAFR) durch gewundenes DNA-Bindungsprotein A

(CbpA) genutzt um mittels Transzytose die Bluthirnschranke zu durchqueren (52,53). Ebenso ist *Neisseria meningitides* ein pathogener Keim, welcher mittels Pili und Oberflächenproteinen wie Adhäsine der Außenmembran (Opa) an den BMEC bindet und durch das Pilin-ähnliche Protein Q (PilQ) zu einer Inflammation und einer erhöhten Permeabilität der Bluthirnschranke führt (52,54). Unser Modell ist limitiert durch den direkten Kontakt der THBMEC und den Bakterien. Um die Mechanismen der Überschreitung der Bluthirnschranke durch die Pathogene zu verstehen, sollten involvierte Signalwege und Proteine detektiert werden. Hierfür wäre es möglich die Zellen aus den Inserts zu ernten und zur weiteren Analyse zu verwenden. Ein weiterer Marker für die Modelle der Bluthirnschranke ist der TEER-Wert. Dieser ist im neu etablierten Modell ungefähr in der Spannweite von üblichen Zellmodellen (20). Dem steht ein Stammzellmodell gegenüber, welches wesentlich höhere Werte erreichen konnte und den physiologischen Bedingungen näher kommt (55,56). Im Modell konnte dies ausgeglichen werden, indem die Anzahl der Bakterien, welche nach 6 Stunden durch die unbehandelten Zellen passieren konnten, die Kontrolle bildete. Durch die Behandlung der THBMEC mit AGE im Modell wurde die Vermutung bestätigt, dass die Glykierung die Permeabilität der Bluthirnschranke erhöht. Ich konnte zeigen, dass diese Effekte nicht durch Einleitung der Apoptose der mikrovaskulären Endothelzellen entstanden, da im MTT-Assay keine Zytotoxizität nachweisbar war. Ebenso blieb der TEER-Wert stabil, sodass die Effekte nicht von einem Zusammenbruch der Bluthirnschranke herrührten. Am ehesten lassen meine Ergebnisse auf eine Beeinflussung des transzellulären und parazellulären Traversal der Bakterien durch die Glykierung schließen. Durch die Nutzung von MGO in einer Konzentration, welche ebenso bei Hyperglykämie im Blut vorkommen könnte (190 +/- 68 nmol/L) (57), kann man vermuten, dass dieser Effekt auch im menschlichen Körper stattfindet und so zu Komplikationen wie einer diabetischen Enzephalopathie führt. Gleichzeitig ist die Aussagekraft des Zellmodells sehr begrenzt, da die Effekte der anderen Zellen der Bluthirnschranke sowie weitere Regulationsmechanismen außer Acht gelassen wurden. Die Behandlung mit Propofol und Noradrenalin wurde ebenfalls mit klinisch relevanten Konzentrationen durchgeführt (45–47). Die Effekte hier konnten ebenfalls nicht durch Zytotoxizität sowie einem Zusammenbruch der Bluthirnschranke erklärt werden. Den schädigenden Effekt von Propofol, welcher in einigen Studien beschrieben wurde (40,41), konnte in meinen Experimenten reproduziert werden, während ich keinen Anhalt für neuroprotektive Effekte (42,43) fand. Die isolierte Behandlung mit

Noradrenalin ergab ebenfalls einen Anstieg des mikrobiellen Traversal. Unter anderen wird eine Dysbalance der Katecholamine als Ursache des Deliriums gesehen (58), jedoch konnten bisherige Studien im Menschen noch kein Zusammenhang zwischen hohen Konzentrationen an Noradrenalin und der Inzidenz für POD finden (59). Die negativen Effekte der Anästhetika wurden im Modell mit den THBMEC durch die Glykierung verstärkt, sodass ich eine mögliche Erklärung für die Korrelation zwischen Diabetes und einem erhöhten Risiko für POD fand. Gleichzeitig könnte dies die Wichtigkeit einer sparsamen Anästhetikaverwendung bei PatientInnen mit Diabetes sowie ein gut eingestelltes Blutzuckerlevel vor Operationen herausstellen.

In meinen Experimenten fokussierte ich mich ausschließlich auf die direkten Einflüsse der AGE und untersuchte die Interaktion mit dem Rezeptor für AGE (RAGE) nicht näher. Diese Bindung beeinflusst ebenfalls die Zellen der Bluthirnschranke, da sie zu vorzeitiger Apoptose, vermehrtem oxidativen Stress oder inflammatorischen Reaktionen im Gewebe (60,61) führt.

Am interessantesten scheint der Effekt der Ascorbinsäure zu sein. Dieses Vitamin beinhaltet die Möglichkeit Glykierung vorzubeugen, was bei Hämoglobin gezeigt werden konnte (62), gleichzeitig birgt es das Risiko selbst als AGE zu fungieren. In meinen Ergebnissen zeigte sich eine teilweise Umkehr der Glykierungseffekte sowie ein vorbeugender Effekt. Patienten nach einer Operation haben ein hohes Level an reaktiven Sauerstoffspezies (ROS), welche oft die Antioxidationskapazität des Körpers übersteigt und so zu Organdysfunktionen führt (63). Auch Hyperglykämie ist mit einem hohen Level an ROS assoziiert (64). Ascorbinsäure ist als einer der wichtigsten Antioxidantien bekannt, welcher den Einfluss der freien Radikale einschränkt (65) und gleichzeitig die Bildung von AGE vorbeugt (66). Meine Ergebnisse konnten zusätzlich zu den bisherigen Erkenntnissen einen Effekt von Ascorbinsäure nach der Glykierung zeigen. Der menschliche Körper ist abhängig von einer adäquaten Aufnahme von Vitamin C, da er nicht in der Lage ist dieses Vitamin selbst herzustellen. Die im Modell verwendeten 0.1 mM Ascorbinsäure ergeben umgerechnet eine realistische Konzentration von 100 mg Ascorbinsäure, welche von einer Person mit einem Blutvolumen von 4-6 L oral aufgenommen wird. Ich vermute, dass ein hohes Level an Ascorbinsäure einen positiven Effekt auf Komplikationen des Diabetes mellitus hat wie beispielsweise die diabetische Enzephalopathie.

3. Literaturverzeichnis

1. Brightman MW, Reese TS. Junctions between intimately apposed cell membranes in the vertebrate brain. *J Cell Biol.* 1969;40(3).
2. Morris AWJ, Sharp MMG, Albargothy NJ, Fernandes R, Hawkes CA, Verma A, et al. Vascular basement membranes as pathways for the passage of fluid into and out of the brain. *Acta Neuropathol.* 2016;131(5).
3. Tilling T, Korte D, Hoheisel D, Galla HJ. Basement membrane proteins influence brain capillary endothelial barrier function in vitro. *J Neurochem.* 1998;71(3).
4. Betz AL, Goldstein GW. Polarity of the blood-brain barrier: Neutral amino acid transport into isolated brain capillaries. *Science (80-).* 1978;202(4364).
5. BRADBURY MWB. Introduction to the Blood-Brain Barrier. Methodology, Biology and Pathology. Edited by WILLIAM M. PARDRIDGE. (Pp. xiv+486; illustrated; f85 hardback; ISBN 0 521 581249.) Cambridge: Cambridge University Press. 1998. *J Anat.* 1999;194(1).
6. Butt AM, Jones HC, Abbott NJ. Electrical resistance across the blood-brain barrier in anaesthetized rats: a developmental study. *J Physiol.* 1990;429(1).
7. Arbanas G. Review of Diagnostic and statistical manual of mental disorders (DSM-5). *Alcohol Psychiatry Res J Psychiatr Res Addict.* 2015;51(1):61–4.
8. Ely EW, Shintani A, Truman B, Speroff T, Gordon SM, Harrell FE, et al. Delirium as a Predictor of Mortality in Mechanically Ventilated Patients in the Intensive Care Unit. *JAMA.* 2004;291(14).
9. Rudolph JL, Ramlawi B, Kuchel GA, McElhaney JE, Xie D, Sellke FW, et al. Chemokines are associated with delirium after cardiac surgery. *Journals Gerontol - Ser A Biol Sci Med Sci.* 2008;63(2).
10. Arshi A, Lai WC, Chen JB, Bukata S V., Stavrakis AI, Zeegen EN. Predictors and Sequelae of Postoperative Delirium in Geriatric Hip Fracture Patients. *Geriatr Orthop Surg Rehabil.* 2018;9.
11. Kratz T, Heinrich M, Schlauß E, Diefenbacher A. The Preventing of Postoperative Delirium. *Dtsch Arztebl Int.* 2015;
12. Laurila JV, Laakkonen ML, Strandberg TE, Tilvis RS. Predisposing and precipitating factors for delirium in a frail geriatric population. *J Psychosom Res.* 2008 Sep 1;65(3):249–54.
13. Morren JA, Manno EM. Neurologic Complications in Critically Ill Patients. *Amin Neurol Gen Med.* 2021 Jan 1;993–1006.
14. du Moulin GC, Paterson D, Hedley-Whyte J, Broitman SA. E. coli peritonitis and bacteremia cause increased blood-brain barrier permeability. *Brain Res.* 1985 Aug 12;340(2):261–8.
15. Jeppsson B, Freund HR, Gimmon Z, James JH, von Meyenfeldt MF, Fischer JE. Blood-brain barrier derangement in sepsis: Cause of septic encephalopathy? *Am J Surg.* 1981;141(1).
16. Stins MF, Badger J, Sik Kim K. Bacterial invasion and transcytosis in transfected human brain microvascular endothelial cells. *Microb Pathog.* 2001;30(1).

17. Hussain M. The Effect of Glycation on the Permeability of an in vitro Blood-brain Barrier Model. [Halle (Saale)]: University Halle - Wittenberg; 2015.
18. Robbins JB, McCracken GH, Gotschlich EC, Ørskov F, Ørskov I, Hanson LA. Escherichia coli K1 Capsular Polysaccharide Associated with Neonatal Meningitis. *N Engl J Med.* 1974;290(22).
19. Kim KS, Itabashi H, Gemski P, Sadoff J, Warren RL, Cross AS. The K1 capsule is the critical determinant in the development of Escherichia coli meningitis in the rat. *J Clin Invest.* 1992;90(3).
20. Srinivasan B, Kolli AR, Esch MB, Abaci HE, Shuler ML, Hickman JJ. TEER Measurement Techniques for In Vitro Barrier Model Systems. Vol. 20, *Journal of Laboratory Automation.* 2015.
21. Schubert-Unkmeir A, Konrad C, Slanina H, Czapek F, Hebling S, Frosch M. Neisseria meningitidis induces brain microvascular endothelial cell detachment from the matrix and cleavage of occludin: A role for MMP-8. *PLoS Pathog.* 2010;6(4).
22. Balda MS, Whitney JA, Flores C, González S, Cereijido M, Matter K. Functional dissociation of paracellular permeability and transepithelial electrical resistance and disruption of the apical-basolateral intramembrane diffusion barrier by expression of a mutant tight junction membrane protein. *J Cell Biol.* 1996;134(4).
23. Harris ES, Nelson WJ. VE-cadherin: At the front, center, and sides of endothelial cell organization and function. Vol. 22, *Current Opinion in Cell Biology.* 2010.
24. Swardfager W, Lanctt K, Rothenburg L, Wong A, Cappell J, Herrmann N. A meta-analysis of cytokines in Alzheimer's disease. *Biol Psychiatry.* 2010;68(10).
25. Gkogkolou P, Böhm M. Advanced glycation end products: Keyplayers in skin aging? Vol. 4, *Dermato-Endocrinology.* 2012.
26. Wu L, Juurlink BHJ. Increased methylglyoxal and oxidative stress in hypertensive rat vascular smooth muscle cells. *Hypertension.* 2002;39(3).
27. Rosca MG, Mustata TG, Kinter MT, Ozdemir AM, Kern TS, Szweda LI, et al. Glycation of mitochondrial proteins from diabetic rat kidney is associated with excess superoxide formation. *Am J Physiol - Ren Physiol.* 2005;289(2 58-2).
28. Lee HJ, Howell SK, Sanford RJ, Beisswenger PJ. Methylglyoxal can modify GAPDH activity and structure. In: *Annals of the New York Academy of Sciences.* 2005.
29. Bennmann D, Horstkorte RD, Hofmann B, Jacobs K, Navarrete-Santos A, Simm A, et al. Advanced glycation endproducts interfere with adhesion and neurite outgrowth. *PLoS One.* 2014 Nov 11;9(11).
30. John WG, Lamb EJ. The maillard or browning reaction in diabetes. *Eye.* 1993;7(2).
31. Schalkwijk CG, Miyata T. Early- and advanced non-enzymatic glycation in diabetic vascular complications: The search for therapeutics. Vol. 42, *Amino Acids.* 2012. p. 1193–204.
32. Van Veen KEB, Brouwer MC, Van Der Ende A, Van De Beek D. Bacterial meningitis in diabetes patients: A population-based prospective study. *Sci Rep.* 2016;6.

33. Kalra S, Zargar A, Jain S, Sethi B, Chowdhury S, Singh A, et al. Diabetes insipidus: The other diabetes. Vol. 20, Indian Journal of Endocrinology and Metabolism. 2016.
34. Schut ES, Westendorp WF, de Gans J, Kruyt ND, Spanjaard L, Reitsma JB, et al. Hyperglycemia in bacterial meningitis: A prospective cohort study. *BMC Infect Dis.* 2009;9.
35. Hussain M, Bork K, Gnanapragassam VS, Bennmann D, Jacobs K, Navarette-Santos A, et al. Novel insights in the dysfunction of human blood-brain barrier after glycation. *Mech Ageing Dev.* 2016;155.
36. Shimizu F, Sano Y, Tominaga O, Maeda T, Abe M aki, Kanda T. Advanced glycation end-products disrupt the blood-brain barrier by stimulating the release of transforming growth factor- β by pericytes and vascular endothelial growth factor and matrix metalloproteinase-2 by endothelial cells in vitro. *Neurobiol Aging.* 2013;34(7).
37. Li Q, Liu H, Du J, Chen B, Li Q, Guo X, et al. Advanced glycation end products induce moesin phosphorylation in murine brain endothelium. *Brain Res.* 2011;1373.
38. Smulter N, Lingehall HC, Gustafson Y, Olofsson B, Engström KG. Delirium after cardiac surgery: Incidence and risk factors. In: *Interactive Cardiovascular and Thoracic Surgery.* 2013.
39. Meredith ME, Qu ZC, May JM. Ascorbate reverses high glucose- and RAGE-induced leak of the endothelial permeability barrier. *Biochem Biophys Res Commun.* 2014;445(1).
40. Doronzio A, Lanni F, Ayrian E, Zhang YP, Bilotta F, Rosa G. Postoperative delirium after anesthesia with propofol, sevoflurane or desflurane: The Pinocchio trial. Interim analysis of safety and preliminary results. *Eur J Anaesthesiol.* 2013;30.
41. Sharma H, Pontén E, Gordh T, Eriksson P, Fredriksson A, Sharma A. Propofol Promotes Blood-Brain Barrier Breakdown and Heat Shock Protein (HSP 72 kd) Activation in the Developing Mouse Brain. *CNS Neurol Disord - Drug Targets.* 2014;13(9).
42. Manataki AD, Tselepis AD, Glantzounis GK, Arnaoutoglou HM, Tsimoyiannis EC, Stavropoulos NE. Lipid peroxidation and the use of emulsified propofol in laparoscopic surgery. In: *Surgical Endoscopy.* 2001.
43. Kubo K, Inada T, Shingu K. Possible role of propofol's cyclooxygenase-inhibiting property in alleviating dopaminergic neuronal loss in the substantia nigra in an MPTP-induced murine model of Parkinson's disease. *Brain Res.* 2011;1387.
44. Ishii K, Makita T, Yamashita H, Matsunaga S, Akiyama D, Toba K, et al. Total intravenous anesthesia with propofol is associated with a lower rate of postoperative delirium in comparison with sevoflurane anesthesia in elderly patients. *J Clin Anesth.* 2016;33.
45. Minami K, Korner MM, Vyska K, Kleesiek K, Knobl H, Korfer R. Effects of pulsatile perfusion on plasma catecholamine levels and hemodynamics during and after cardiac operations with cardiopulmonary bypass. *J Thorac Cardiovasc Surg.* 1990;99(1).

46. Takizawa E, Hiraoka H, Takizawa D, Goto F. Changes in the effect of propofol in response to altered plasma protein binding during normothermic cardiopulmonary bypass. *Br J Anaesth.* 2006;96(2).
47. Wessen A, Persson PM, Nilsson A, Hartvig P. Concentration-effect relationships of propofol after total intravenous anesthesia. *Anesth Analg.* 1993;77(5).
48. DeBault LE, Cancilla PA. γ -glutamyl transpeptidase in isolated brain endothelial cells: Induction by glial cells in vitro. *Science* (80-). 1980;207(4431).
49. Ohtsuki S. IC. UY. SY. MF. GF. DX. SJM. CPO. KY. TM. & TT. Quantitative targeted absolute proteomic analysis of transporters, receptors and junction proteins for validation of human cerebral microvascular endothelial cell line hCMEC/D3 as a human blood-brain barrier model. *Mol Pharm* 10(1). 2013;289–96.
50. Janzer RC, Raff MC. Astrocytes induce blood-brain barrier properties in endothelial cells. *Nature.* 1987;325(6101).
51. Ramsauer M, Krause D, Dermietzel R. Angiogenesis of the blood-brain barrier in vitro and the function of cerebral pericytes. *FASEB J.* 2002;16(10).
52. Al-Obaidi MMJ, Desa MNM. Mechanisms of Blood Brain Barrier Disruption by Different Types of Bacteria, and Bacterial–Host Interactions Facilitate the Bacterial Pathogen Invading the Brain. Vol. 38, *Cellular and Molecular Neurobiology.* 2018.
53. Iovino F, Orihuela CJ, Moorlag HE, Molema G, Bijlsma JJE. Interactions between Blood-Borne *Streptococcus pneumoniae* and the Blood-Brain Barrier Preceding Meningitis. *PLoS One.* 2013;8(7).
54. Pron B, Taha MK, Rambaud C, Fournet JC, Pattey N, Monnet JP, et al. Interaction of *Neisseria meningitidis* with the Components of the Blood-Brain Barrier Correlates with an Increased Expression of Pili. *J Infect Dis* [Internet]. 1997 Nov 1;176(5):1285–92. Available from: <https://doi.org/10.1086/514124>
55. Lippmann ES, Azarin SM, Kay JE, Nessler RA, Wilson HK, Al-Ahmad A, et al. Derivation of blood-brain barrier endothelial cells from human pluripotent stem cells. *Nat Biotechnol.* 2012;30(8).
56. Cecchelli R, Aday S, Sevin E, Almeida C, Culot M, Dehouck L, et al. A stable and reproducible human blood-brain barrier model derived from hematopoietic stem cells. *PLoS One.* 2014;9(6).
57. Dhananjayan K, Irrgang F, Raju R, Harman DG, Moran C, Srikanth V, et al. Determination of glyoxal and methylglyoxal in serum by UHPLC coupled with fluorescence detection. *Anal Biochem.* 2019;573.
58. Henjum K, Godang K, Quist-Paulsen E, Idland AV, Neerland BE, Sandvig H, et al. Cerebrospinal fluid catecholamines in delirium and dementia. *Brain Commun.* 2021;3(3).
59. Yasuda Y, Nishikimi M, Nishida K, Takahashi K, Numaguchi A, Higashi M, et al. Relationship Between Serum Norepinephrine Levels at ICU Admission and the Risk of ICU-Acquired Delirium: Secondary Analysis of the Melatonin Evaluation of Lowered Inflammation of ICU Trial. *Crit Care Explor.* 2020;2(2).

60. Warboys CM, Toh HB, Fraser PA. Role of NADPH oxidase in retinal microvascular permeability increase by RAGE activation. *Investig Ophthalmol Vis Sci.* 2009;50(3).
61. Chen B hua, Jiang D yong, Tang L sheng. Advanced glycation end-products induce apoptosis involving the signaling pathways of oxidative stress in bovine retinal pericytes. *Life Sci.* 2006;79(11).
62. Krone CA, Ely JTA. Ascorbic acid, glycation, glycohemoglobin and aging. *Med Hypotheses.* 2004;62(2).
63. Roy J, Galano JM, Durand T, Le Guennec JY, Lee JCY. Physiological role of reactive oxygen species as promoters of natural defenses. Vol. 31, *FASEB Journal.* 2017.
64. Volpe CMO, Villar-Delfino PH, Dos Anjos PMF, Nogueira-Machado JA. Cellular death, reactive oxygen species (ROS) and diabetic complications review-Article. *Cell Death Dis.* 2018;9(2).
65. Frei B, England L, Ames BN. Ascorbate is an outstanding antioxidant in human blood plasma. *Proc Natl Acad Sci U S A.* 1989;86(16).
66. Vinson JA, Howard TB. Inhibition of protein glycation and advanced glycation end products by ascorbic acid and other vitamins and nutrients. *J Nutr Biochem.* 1996;7(12).

4. Thesen

1. Die Etablierung des Zellmodells mit „Transfected human brain endothelial cells“ im Labor erfolgte mit direkter Bestimmung des mikrobiellen Traversals an der Bluthirnschranke zur Quantifizierung der Permeabilität.
2. In den „Transfected human brain endothelial cells“ sind die wesentlichen Merkmale der zerebralen mikrovaskulären Endothelzellen erhalten, was mittels Westernblot durch Proteinbestimmungen der Tight- und Adherens-Junctions und Nachweis der Reaktion auf proinflammatorische Signale gezeigt wurde.
3. Die Glykierung der „Transfected human brain endothelial cells“ mittels Methylglyoxal in physiologischen Konzentrationen erhöht das mikrobielle Traversal im Modell.
4. Die Behandlung der „Transfected human brain endothelial cells“ mit Propofol und Noradrenalin in klinisch relevanten Konzentrationen erhöhen das mikrobielle Traversal im Modell.
5. Die Anwendung von Ascorbinsäure vor und nach der Behandlung der „Transfected human brain endothelial cells“ mit Methylglyoxal vermindert und macht die Einflüsse der Glykierung teilweise rückgängig an der Bluthirnschranke ohne selbst das mikrobielle Traversal im Modell zu erhöhen.
6. Die Ergebnisse lassen vermuten, dass Glykierung, Propofol und Noradrenalin die Permeabilität der Bluthirnschranke für mikrobielle Erreger erhöht und so die Inzidenz für Pathologien wie Sepsis, Meningitis und Postoperatives Delirium erhöht.
7. Eine adäquate Aufnahme und Konzentration an Ascorbinsäure könnte einen positiven Effekt auf Komplikationen des Diabetes haben durch Verhinderung der Glykierung von Proteinen im menschlichen Organismus.
8. Die Ergebnisse lassen auf die Wichtigkeit einer sparsamen Anästhetikaverwendung bei PatientInnen mit Diabetes sowie ein gut eingestelltes Blutzuckerlevel vor Operationen schließen, um postoperative Pathologien durch eine erhöhte Durchlässigkeit der Bluthirnschranke zu vermeiden.

Publikationsteil

1. Paper:

Weber, V., Bork, K., Horstkorte, R., Olzscha, H. Analyzing the Permeability of the Blood-Brain Barrier by Microbial Traversal through Microvascular Endothelial Cells. *J. Vis. Exp.* (156), e60692, doi:10.3791/60692 (2020).

Abdruck mit freundlicher Genehmigung des Verlags ‚JoVe‘ vom 21.11.2023

Geleistete Beiträge: Anteil an der Konzeptualisierung, Formale Analyse, Schreiben des originalen Entwurfes, Anteil am Review und Bearbeitung, Visualisierung.

2. Paper:

Weber, V.; Olzscha, H.; Längrich, T.; Hartmann, C.; Jung, M.; Hofmann, B.; Horstkorte, R.; Bork, K. Glycation Increases the Risk of Microbial Traversal through an Endothelial Model of the Human Blood-Brain Barrier after Use of Anesthetics. *J. Clin. Med.* 2020, 9, 3672. <https://doi.org/10.3390/jcm9113672>.

Abdruck mit freundlicher Genehmigung des Verlags ‚MDPI‘ vom 12.12.2023

Geleistete Beiträge: Anteil an der Konzeptualisierung, Anteil an der formalen Analyse, Anteil am Schreiben des originalen Entwurfes, Anteil am Review und Bearbeitung, Visualisierung.

Analyzing the Permeability of the Blood-Brain Barrier by Microbial Traversal through Microvascular Endothelial Cells

AUTHORS AND AFFILIATIONS:

Veronika Weber¹, Kaya Bork¹, Rüdiger Horstkorte¹, Heidi Olzscha¹

¹Institute of Physiological Chemistry, Martin Luther University Halle-Wittenberg, Halle (Saale), Germany

Corresponding Author:

Heidi Olzscha (heidi.olzscha@medizin.uni-halle.de)

Email Addresses of Co-authors:

Veronika Weber (veronika.weber@uk-halle.de)

Kaya Bork (kaya.bork@medizin.uni-halle.de)

Rüdiger Horstkorte (ruediger.horstkorte@medizin.uni-halle.de)

KEYWORDS:

bacterial traversal, blood-brain barrier, cellular adherence, compound screening, endothelial cells, inflammation, meningitis, cellular permeability, postoperative delirium, tight junctions, transfected human brain microvascular endothelial cells

SUMMARY:

The human blood-brain barrier selectively prevents penetration of hydrophilic molecules and pathogens into the brain. Several pathologies, including meningitis and postoperative delirium, are associated with an increased permeability of the blood-brain barrier. Here, we describe an endothelial cell culture model to test the barrier permeability by microbial traversal.

ABSTRACT:

The human blood-brain barrier (BBB) is characterized by a very low permeability for biomolecules in order to protect and regulate the metabolism of the brain. The BBB is

mainly formed out of endothelial cells embedded in collagen IV and fibronectin-rich basement membranes. Several pathologies result from dysfunction of the BBB followed by microbial traversal, causing diseases such as meningitis. In order to test the effect of multiple parameters, including different drugs and anesthetics, on the permeability of the BBB we established a novel human cell culture model mimicking the BBB with human brain microvascular endothelial cells. The endothelial cells are grown on collagen IV and fibronectin-coated filter units until confluence and can then be treated with different compounds of interest. In order to demonstrate a microbial traversal, the upper chamber with the apical surface of the endothelial cells is inoculated with bacteria. After an incubation period, samples of the lower chamber are plated on agar plates and the obtained colonies are counted, whereby the number of colonies correlate with the permeability of the BBB. Endogenous cellular factors can be analyzed in this experimental set-up in order to elucidate basic cellular mechanisms of the endothelial cells contributing to the BBB. In addition, this platform allows performing a screen for compounds that might affect the permeability of the endothelial cells. Finally, bacterial traversal can be studied and linked to different pathologies, such as meningitis. It might be possible to extend the model and analyze the pathways of the bacteria through the BBB. In this article, we provide a detailed protocol of the described method to investigate the permeability of the BBB.

INTRODUCTION:

The human BBB is a unique boundary of brain tissue, separating the brain from the blood. It strictly regulates the passage of larger and hydrophilic molecules, blocks paracellular diffusion, and maintains brain homeostasis. It also protects the brain from plasma fluctuations, toxins, microbes, and guides inflammatory cells as part of the central nervous system (CNS) immunity. Since its discovery a century ago¹, many studies have been carried out to understand the structure and function of the BBB. The complex interactions of cells, proteins, and signals from brain and blood demand still further investigation and models.

The human BBB is composed of three cell types: brain microvascular endothelial cells (BMECs), pericytes, and astrocytes^{2,3}. The BMECs differ from the majority of the endothelial cells in the body in that they possess a high number of tight junctions and adherens junctions⁴, low pinocytotic activity^{2,5}, and a continuous basement membrane^{6,7} to block paracellular diffusion. Small lipophilic molecules can diffuse and pass the BBB following their concentration gradient; larger and hydrophilic molecules enter or leave

the brain only through polarized expressed selective transport systems⁸. This regulation results in a high transendothelial electrical resistance (TEER) of 1,500-2,000 $\Omega \cdot \text{cm}^2$ that is inversely correlated to permeability^{9,10}. Although BMECs build a tight barrier, they can react to local and peripheral signals^{11,12}. There is a close interaction between BMECs and astrocytes¹³; the astrocyte end-feet build a layer around the vessels and induce the formation of tight junctions^{13,14}. They are involved in BBB maturation with different factors, including transforming growth factor- β (TGF- β)^{15,16}. In addition, pericytes play a key role in the regulation of angiogenesis¹⁷ and preventing apoptosis of the endothelium in cellular differentiation¹⁸ (Figure 1). They are embedded in the basement membrane and provide structural stability of the vessel wall¹⁹.

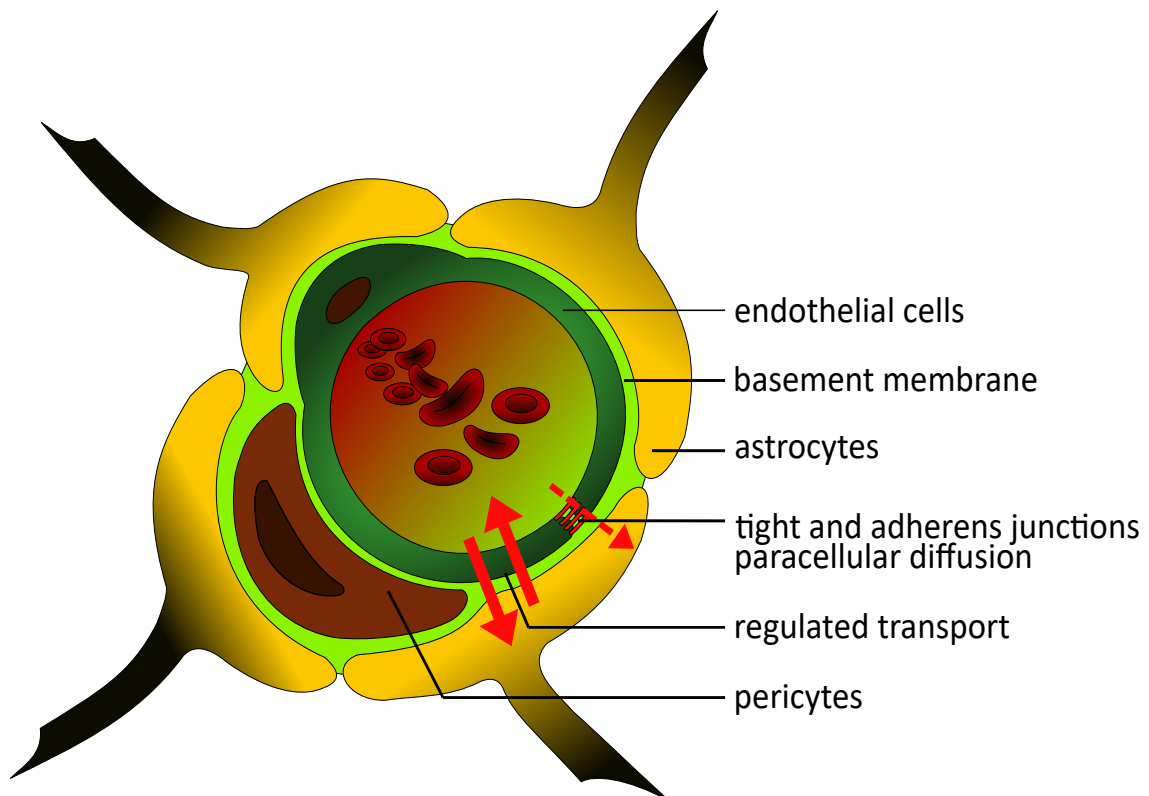


Figure 1: Schematic structure of the blood-brain barrier.

The unique structure of the human BBB is composed of three different cell types. The microvessel lumen is surrounded by endothelial cells, which are enriched in tight junctions, and are not fenestrated. They are embedded in the basement membrane, like the pericytes. These cells are important for structural stability of the vessel wall and play a role in the development of the BBB next to the astrocytes. Their end-feet build a close layer around the vessel and support the building of tight junctions. All components of the BBB are important for physiological functionality.

Many different pathologies are related to the collapse of the BBB (e.g., septic encephalopathy). The affected patients have increased protein levels in the

cerebrospinal fluid²⁰, and the brain parenchyma in affected rodents shows an increased uptake of marked colloidal iron oxide and amino acids^{21,22}. These results point towards an increased permeability of the BBB that occurs alongside an increased pinocytosis in BMECs²¹ and endothelial activation²³. Another associated pathology related to an altered BBB is meningitis, a medical emergency and a complex inflammation accompanied with cerebral edema that can lead to neuronal cell death. The primary entry site of circulating bacteria is supposed to be the microvessels²⁴; however, the BBB prevents the entry of bacteria. The permeability of the BBB is not always linked to an increase in experimental hematogenous meningitis²⁵ and the mechanisms can be multifactorial. Coincidence of sepsis with postoperative delirium (POD)²⁶ and the association with preoperative infections^{27,28} indicates the need for a BBB model that enables the direct exposure to bacteria to get a better understanding into bacterial pathogenesis.

There are many gaps in understanding and quantifying the microbial traversal through the BBB. Therefore, we developed a model that allows a convenient testing of different factors and conditions with a direct correlation between bacterial traversal and influences on the permeability of the BBB. Previous work focused on the paracellular permeability and included TEER measurement and tracer flux. In addition, macromolecule transport was analyzed by conjugated molecules or antibodies, whereby different models using only endothelial cells or combinations with astrocytes and pericytes were developed. Due to the difficulty in obtaining human tissue on a regular basis, many animal-based models are used. Brain endothelial cells of bovine and porcine origin form tight monolayers with a high TEER that form well-shaped apical-basal polarity and are suited for investigations of small molecule transport through the BBB. The proteins differ in sequence from their human homologues^{29,30}, making investigation of therapeutic antibodies difficult. For this reason, murine or human culture models may be preferable. Mouse or rats as sample sources have the advantage of being obtained from well characterized species but yield few cells for study purposes. This can be circumvented by the use of immortalized mouse brain endothelioma (END) cell lines bEND.3, bEND.5 or cEND³¹⁻³³.

Primary cultured cells from human tissue are difficult to obtain and to handle on a regular basis. Therefore, most human cellular models used in research investigating the human BBB are immortalized endothelial cell lines. A published cell line is human cerebral microvascular endothelial cell line hCMEC/D3, which is well suited for studying

drug uptake and is easy to handle. The cells build a monolayer and express the characteristic tight junction proteins of the BBB³⁴, whereas the expression level of claudin-5 is reported to be lower than in intact microvessels³⁵ and many specific transporters have been detected at transcript level³⁶ as well as in proteomic studies³⁴. A relatively low TEER in the range of 30–50 $\Omega \cdot \text{cm}^2$ is still a challenge³⁷. Another source for brain endothelial cells are human pluripotent stem cells (hPSCs)³⁸ and human cord blood-derived stem cells of circulating endothelial progenitor and hematopoietic lineages^{39,40}. Both protocols of differentiation result in tight cell monolayers and high TEER values (e.g., 1,450 $\Omega \cdot \text{cm}^2$ in co-cultures)³⁸. These stem cell models require extreme care for cultivation, yet offer the opportunity to study the influence of regulating hormones⁴¹ or diseases with genetic backgrounds⁴² on BBB development.

In this study, we established an immortalized transfected human brain microvascular endothelial cell line, THBMEC,⁴³ to mimic the BBB and to study bacterial traversal. Cells are seeded on a filter and grown to 100% confluency in this cell culture model. Bacteria are inoculated in the upper part of the cell culture chamber. We use *Escherichia coli* (*E. coli*) in our sample study because of the high incidence of *E. coli* meningitis⁴⁴. It has been shown that the lowest permeability of cell monolayer occurs between day 13 and day 15 after seeding⁴⁵. Therefore, treatment of the THBMEC monolayer is performed after this time and bacteria are inoculated afterwards in the medium on the apical surface of the monolayer. After an incubation time, bacteria that were able to cross the barrier are quantified via plating medium with the bacteria on agar plates and counting the colonies. An increased number of colonies correlates with higher bacterial traversal through the BBB. The TEER is about 70 $\Omega \cdot \text{cm}^2$,⁴⁶. However, it is not necessary to measure the TEER in the described method. Although it is a well-established value for the permeability of the BBB, it seems to have no impact on the traversal of bacteria through the BBB. Untreated cells serve as a control of tightness in our model. It has been shown in previous work that the cells are able to react to proinflammatory cytokines and express typical tight junction proteins⁴⁷. This allows for compound screening and validation of a larger set of transporter substrates and receptors.

PROTOCOL:

1. Preparation of Buffer and Reagents

1.1. Prepare 10x phosphate buffer saline (10x PBS) by adding 80 g of sodium chloride (NaCl), 2 g of potassium chloride (KCl), 14.4 g of disodium-hydrogen-

phosphate dihydrate ($\text{Na}_2\text{HPO}_4 \cdot 2\text{H}_2\text{O}$) and 2 g of potassium-dihydrogen phosphate (KH_2PO_4) in a 1 L glass flask in 1 L of double distilled H_2O . Autoclave the 10x PBS solution and dilute 100 mL of this solution in 900 mL of double distilled water to get 1x PBS.

1.1.1. Use the autoclave to sterilize solutions. Put the glass flask into the basket, close the lid and sterilize it for 15 min at 121 °C and 98.9 kPa.

NOTE: This protocol is always used for autoclaving solutions in further steps.

1.2. Prepare a 10 µg/mL collagen IV and 10 µg/mL fibronectin solution by diluting 0.5 mg/mL fibronectin solution and the 0.3 mg/mL collagen IV solution each with 1x PBS to 100 mg/µL aliquots in 1.5 mL micro tubes. Thereafter, mix 100 µL of both aliquots with 1,800 µL of 1x PBS in 2 mL micro tubes and store them at -20 °C.

1.3. Prepare DMEM/F-12 medium by adding 4% fetal bovine serum and 2 mM L-glutamine and 100 mg/L penicillin/streptomycin to the medium and store it at 4 °C.

1.4. Prepare 1x trypsin-EDTA solution by diluting 5 mL of the 10x concentrated trypsin-EDTA solution with 45 mL of 1x PBS in a 50 mL tube and store it at 4 °C.

1.5. Prepare 500 mL of LB medium by weighing 10 g of LB broth base in a 500 mL glass flask. Add 500 mL of sterilized water and autoclave it.

1.6. Prepare LB agar by weighing 10 g of LB broth base and 7.5 g of agar-agar in a 500 mL glass flask. Add 500 mL of sterilized water before autoclaving and do not close the lid of the flask. Autoclave and leave the solution to cool down until it is warm to the touch.

1.7. Prepare antibiotic-free medium by adding 4% fetal bovine serum and 2 mM L-glutamine, but no penicillin/streptomycin to the DMEM/F-12 medium and store it at 4 °C as in step 1.3.

2. Growth of the Blood-brain Barrier Mimicking Cells

2.1. To assemble the 12 well plate, put the cell culture inserts into the wells (**Figure 2A**).

2.1.1. Unpack the plate and each insert in a biological safety cabinet and perform further steps there. Use sterilized forceps to grab the insert at its broad base to move it.

2.2. Coat the porous membrane of each insert with 90 μL of 10 $\mu\text{g}/\text{mL}$ collagen IV and 10 $\mu\text{g}/\text{mL}$ fibronectin mixture. Incubate the 12 well plate for 24 h at 37 °C in a cell culture incubator (**Figure 2B**).

2.3. Wash the inserts twice by pipetting 1 mL of 1x PBS into each insert and aspirate the solution with a vacuum pump for cell cultures.

2.4. Equilibrate the membranes by pipetting 0.5 mL of prewarmed DMEM/F-12 medium in the upper and 1.5 mL in the lower chamber. Incubate the plate for 30 min at 37 °C in a cell culture incubator with 5% CO_2 atmosphere (**Figure 2C**).

2.5. Seed 2×10^5 human microvascular endothelial cells into each upper chamber and incubate the 12 well plate at 37 °C in a cell culture incubator (**Figure 2D**).

2.5.1. Aspirate the medium from the cell culture flask using a vacuum pump for cell cultures and wash the monolayer by pipetting 10 mL of 1x PBS and aspirating the solution afterwards with a vacuum pump.

2.5.2. Cover the cells completely with 1x concentrated trypsin-EDTA by pipetting 5 mL of the solution into the cell culture flask. Incubate the flask for 3–5 min at 37 °C in a cell culture incubator.

NOTE: If the cells are not dissociated, firmly tap the flask against the palm of the hand to dislodge the cells.

2.5.3. Take 5 mL with a pipette as an aliquot from the cell suspension in a 15 mL tube and add 5 mL of the FCS-containing medium to stop the enzymatic reaction.

2.5.4. Centrifuge the suspension for 3 min at $210 \times g$, remove the supernatant with a vacuum pump, and resuspend the pellet in 5 mL of medium with a pipette.

2.5.5. Use the cell counter by mixing 10 μL of the cell suspension with 10 μL of 0.4% trypan blue stain in a 1.5 mL micro tube. Add 10 μL of the mixture into a counting chamber slide, put it into the cell counter, and start counting.

2.5.5.1. Focus the counter on the cells so that their edge is dark blue and the middle white. Thereafter, start the appropriate program for cell counting.

2.5.6. To calculate the volume for each insert, divide the obtained 2×10^5 cells per insert with the calculated concentration of the cell suspension.

3. Cultivation of the Blood-brain Barrier Model

- 3.1. Incubate the 12 well plate for 14 days at 37 °C.
- 3.2. Change 0.5 mL of medium for the upper chamber and 1.5 mL of medium for the lower one every 2–3 days. Warm the medium before putting it in the cell flask. Aspirate with the vacuum pump (**Figure 2E**).

NOTE: Work carefully to avoid touching the membrane.

- 3.3. Check the status of the cells by imaging them with a microscope and determine the confluency. Ensure that the confluency is 100% after 14 days.

4. Preparation of Bacteria

- 4.1. A day before measurement, put a colony of the *E. coli* strain GM2163 into LB medium. Incubate the culture tube for 24 h at 37 °C with 180 rpm in an incubation shaker (**Figure 2F**).

- 4.1.1. Cultivate the *E. coli* strain on an LB agar plate at 4 °C. Take one colony with a sterilized pick and put the pick in the prepared culture tube with 3 mL of LB medium.

- 4.1.2. Prepare an LB agar plate for each insert with warm LB agar solution and fill the Petri dishes to half their total volume. Let them become solid and store them at 4 °C.

5. Treatment of Cells

- 5.1. On day 14 after seeding, treat cells with compounds or measure the transendothelial electrical resistance (TEER), if planned (**Figure 2G**).

NOTE: Always have some untreated cells as a control.

- 5.1.1. To treat cells with the compound of interest, dilute the compound to the final concentration in DMEM/F-12 medium. Add 0.5 mL of this mixture into the upper chamber and 1.5 mL into the lower chamber. Incubate the plate in a cell culture incubator for the desired time.

- 5.2. Afterwards, exchange the complete medium with antibiotic-free medium by aspirating with the vacuum pump and pipetting (**Figure 2H**).

6. Measurement of Permeability

- 6.1. To get constant concentrations of bacteria, measure the optical density with a photometer at a wavelength of 600 nm. Dilute the overnight solution of bacteria with LB medium in a 50 mL falcon tube to an OD₆₀₀ of 0.5 ± 0.05. Work on ice.

6.1.1. Fill 1 mL of LB medium into a cuvette. Start the photometer and put the cuvette in, marked side forward. Press the bottom "**Blank**" for measuring the blank value afterwards.

6.1.2. Measure the density of the bacterial solution by filling it into a cuvette, putting it in, and pressing the bottom sample. Repeat the measurement during the diluting until obtaining the final concentration.

6.2. Work in a biological safety cabinet where bacteria can be handled with the prepared 12 well plate and bacterial solution at $OD_{600} = 0.5$. Add 450 μL of bacterial solution only into each upper chamber containing 0.5 mL of medium (**Figure 2I**).

6.3. Incubate the 12 well plate for 6 h at 37 °C in an incubator.

NOTE: The protocol dictates to pause here.

6.4. Sample 50 μL of the medium with a pipette from each lower chamber by removing the insert with forceps (**Figure 2J**). Take care not to spill the medium from the upper chambers to the lower ones.

6.5. Plate each sample on a separate agar-plate (**Figure 2K**). Drop the sample on the plate and streak out the solution with a cell spreader.

6.6. Incubate the agar plates for 24 h at 37 °C in an incubator.

6.7. Count the colonies in each plate (**Figure 2L**).

7. Analyzing Data

7.1. Write the data in a table and calculate the average and standard deviation of the observed colonies of treated and untreated cells.

7.2. Display the average as the absolute number of colonies.

7.2.1. To normalize the results, calculate the relative number of colonies by dividing all results with the control value.

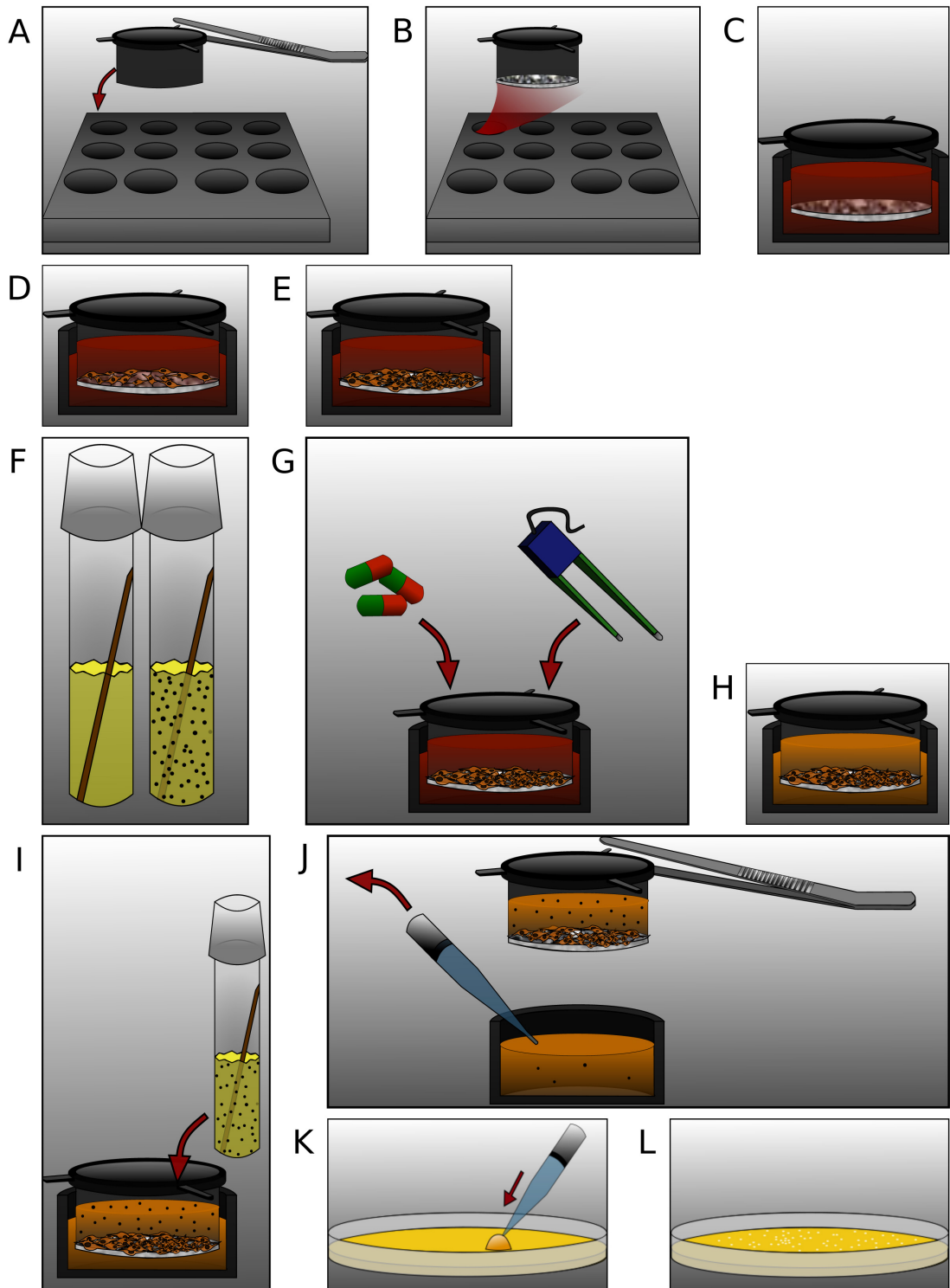


Figure 2: Detailed presentation of the individual steps in the protocol.

(A) Put the inserts with sterilized forceps into the 12 well plate. (B) Coat each insert with 90 μL of fibronectin and collagen IV mixture and incubate for 24 h. (C) Equilibrate the membranes with prewarmed medium for 30 min. (D) Seed 2×10^5 human brain microvascular endothelial cells per insert. (E) Cultivate the plate for the appropriate amount of time. (F) One day before measuring, put an *E. coli* colony into a LB medium

culture tube and incubate for 24 h. **(G)** Treat cells or measure TEER. **(H)** Exchange complete medium with antibiotic-free medium. **(I)** Add 450 μL of bacterial solution ($\text{OD}_{600} = 0.5$) into each upper chamber and incubate for 6 h. **(J)** Sample 50 μL of medium from each lower chamber removing insert with forceps. **(K)** Plate the sample on agar plates and incubate for 24 h. **(L)** Count the colonies and analyze the data.

REPRESENTATIVE RESULTS:

Following the protocol, the cells were seeded, and the BBB model was built. At day 14 after seeding, the cells were treated with glyoxal as a reactive aldehyde. The aim of the experiment was to investigate the correlation between age and diabetes in POD^{27} and the high incidence of meningitis in elderly patients⁴⁸. The increased levels of advanced glycation end products (AGEs) in both age and diabetes⁴⁹ demand further examination of the effect of glycation in the pathogenesis of microbial traversal through the BBB. Glycation is a non-enzymatic reaction of free amino groups in proteins with carbonyl groups of reducing carbohydrates or other carbonyl compounds. Glucose is well known as donor of carbonyl groups; however, there are more reactive ones known. After building an unstable Schiff's base, they rearrange to more stable and reactive dicarbonyl compounds like glyoxal. AGEs, the final products, can cause crosslinks between proteins⁵⁰. They can damage cellular structures and alter cellular function by interaction with the receptor of AGEs (RAGE)⁵¹.

Cells were treated with a 0.05 and 0.15 mM glyoxal (GO) solution for 1 h, and untreated cells served as a control. Glycation was detected via immunoblotting and detection with an anti-AGE antibody (**Figure 3**). The obtained bacterial colonies were counted and represented as the absolute number of colonies (**Figure 4A**) or the relative number of colonies normalized to the control (**Figure 4B**). The medium taken from wells with the untreated cells formed very few colonies. This result demonstrated that the untreated cells were able to build a barrier and could serve as a control. Samples treated with glyoxal displayed an increased number of colonies, leading to the conclusion that there is an effect of glyoxal on the THBMECs and the cellular barrier density, because the number of colonies demonstrated a significant difference between untreated and treated cells. The increased bacterial crossing of the barrier after the treatment with glyoxal could explain why diabetes is correlated to diseases with a BBB breakdown.

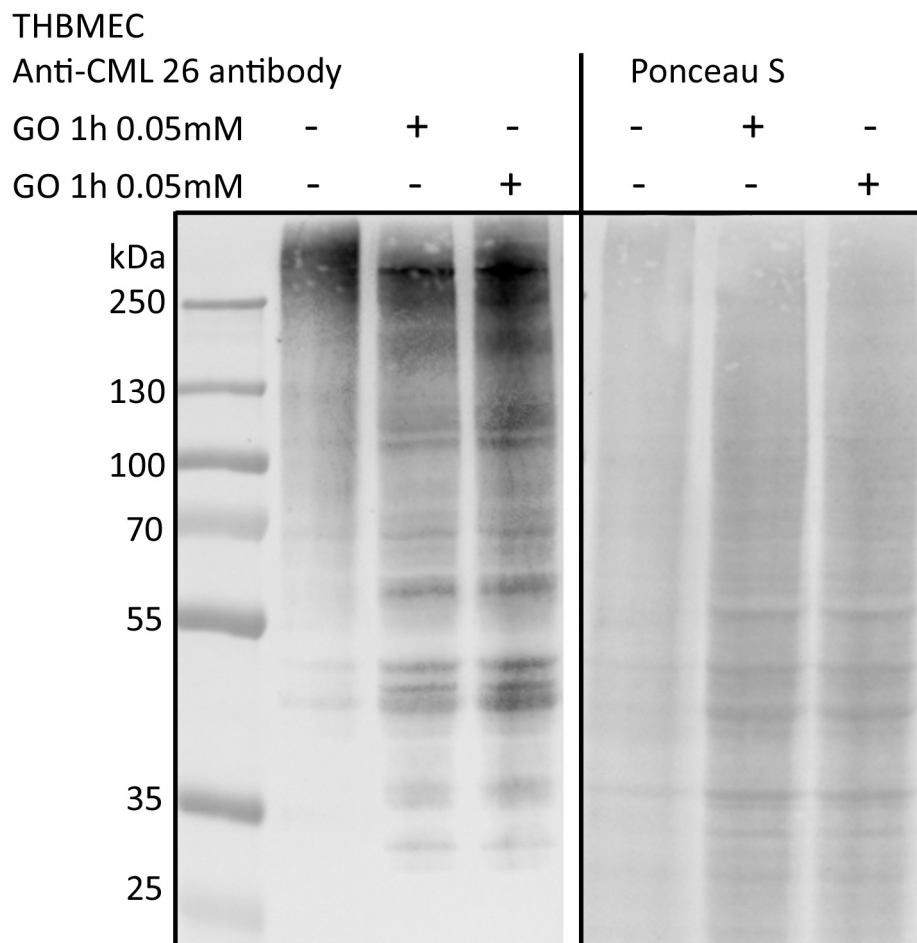


Figure 3: Detection of protein glycation via immunoblotting.

THBMECs were treated with GO at different concentrations for 1 h. Total protein was isolated and separated using SDS-PAGE. Glycation of the proteins was detected via immunoblotting using anti-AGE-antibody (CML-26).

In a different setting, protein glycation of THBMECs was induced by glucose. Sterilized glucose was added to the DMEM/F-12 medium to increase glucose concentration from normal glucose medium (NG) with 17.5 mM to high glucose medium (HG) with 42.5 mM. THBMECs were cultivated in two different cell culture flasks: one in normal glucose (NG) medium and the other in high glucose (HG) medium. These two different media were also used for growth of the BBB on filters in 12 well plates. Cells cultivated in NG medium served as a control. The obtained colonies are represented as the absolute number of colonies (**Figure 4C**) or the relative number of colonies normalized to the control (**Figure 4D**). The results indicate no significant effect on the traversal of bacteria through the human BBB, leading to the conclusion that the effect of NG vs. HG

was not severe enough to affect the integrity of the BBB. The different scenarios were designed to prove the model and the integrity of the cells mimicking the BBB.

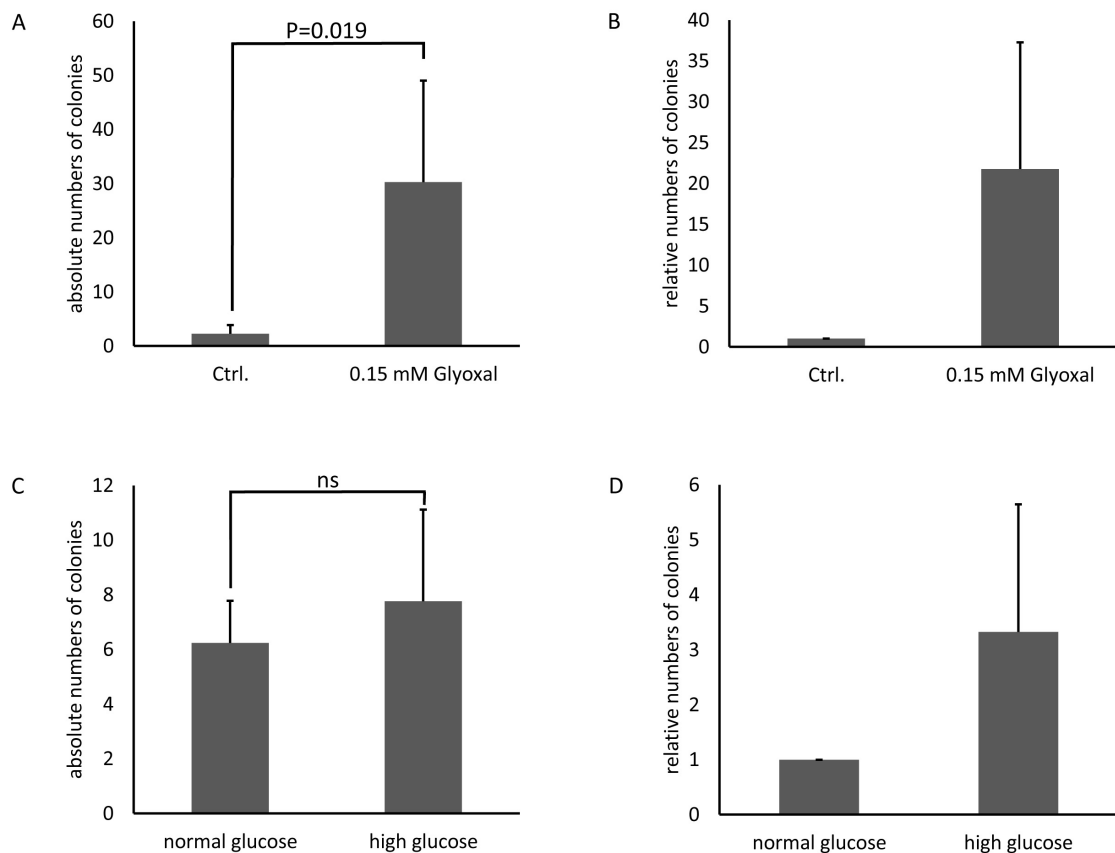


Figure 4: Absolute and relative numbers of counted bacterial colonies in the BBB model with THBMECs.

THBMECs were treated with 0.15 mM GO for 1 h, untreated cells served as a control. A total of 450 μ L of *E. coli* suspension ($OD_{600} = 0.5$) was added to each upper chamber. Medium from the lower chambers was plated on agar plates after 6 h. **(A)** The graph shows the average mean \pm SEM of counted colonies. **(B)** The graph shows the counted colonies normalized to the untreated cells as control \pm SEM ($n = 4$). In **(C)** and **(D)**, THBMECs were cultivated in NG and HG medium. A total of 450 μ L of *E. coli* suspension ($OD_{600} = 0.5$) was added to each upper chamber. Medium from the lower chamber was plated on agar plates after 6 h. **(C)** The graph shows the average mean \pm SEM of counted colonies. **(D)** The graph shows the counted colonies normalized to the untreated cells as control \pm SEM ($n = 3$).

DISCUSSION:

Limited insight into the pathogenesis of microbial traversal limits further development of therapies for POD or meningitis. The mortality and morbidity of these diseases demand better patient treatment, require research of the underlying mechanisms, and need a

robust platform for compound screening. The multifactorial events can be studied with human BMECs. Several successful reported isolation procedures of BMECs from a number of species have shown a loss of the cells' characteristic molecular signature^{52,53}. The described THBMECs in this procedure were transfected in very early passages, where they exhibited specific brain endothelial cell characteristics and preserved them⁴³. This is important, because not all steps in the affected pathways have been discovered so far, and this model seems to mimic conventional BMECs. Our presented model shows direct influences on BMECs and the microbial traversal through the BBB.

The handling of THBMEC cells is straightforward, and the required technical equipment exists in most life science laboratories. Our model allows for an immediate start of investigative procedures after the THBMECs have built a tight monolayer. The field of applications can be extensive because of the possible combinations between new tests and conventional assays such as TEER measurement or labeling with tracers⁵⁴. It is also possible to add astrocytes or pericytes to make a co- or triple-culture model. The influence of drugs on the microbial traversal could also be tested in our model by treating the THBMECs with compounds before inoculating the upper chamber with bacteria. In fact, it is possible to purchase inserts with filters for 96 well plates allowing the automation of the procedure. This can facilitate the implementation of high-throughput drug screening systems to accelerate the discovery of drugs against the mentioned diseases and to reduce side effects on the BBB during drug development.

A critical step in the presented method is the incubation time after adding the bacteria to the upper chamber. It is important to use hours as timelines in the protocol, because the generation time of *E. coli* is only 20 min⁵⁵. Otherwise, use of different time points could lead to misleading results. There is also a possible risk of contamination between upper and lower chamber during the bacterial exposure if the plates are not handled with care. Any alterations to the 12 well plate at this point could contaminate the medium in the lower chamber.

E. coli is one well-known, very common cause of bacterial meningitis. Further investigations should test different bacteria that are also associated with meningitis, such as *Neisseria meningitidis*⁵⁶ or *Streptococcus pneumoniae*⁵⁷. These seem to use different mechanisms to cross the BBB and need to be better understood for the treatment of patients. In elderly patients, the incidence for POD increases²⁶ as well as the number of occurring comorbidities. It is known that there are interactions between

different diseases, especially systemic ones like diabetes. In our model, it is possible to simulate those conditions or treat the cells before adding the bacteria.

The model is limited by the direct contact of THBMECs and bacteria, and further research is necessary to investigate potential mechanisms of contact to detect the involved pathways and proteins. However, it is possible to remove inserts and harvest the cells for further analysis. The TEER of the model is lower in comparison to stem cell models³⁸⁻⁴⁰. We confirmed this by using a bacterial concentration that did not cross the BBB in untreated cells after 6 h.

In summary, this method represents a robust platform to analyze the traversal of bacteria through the BBB with the potential to expand it for high-throughput drug screenings.

ACKNOWLEDGMENTS:

The authors acknowledge Dr. Maryam Hussain for previous work on this method, the group of PD Dr. Kerstin Danker (Charité-Universitätsmedizin, Berlin) for providing the THBMECs and Juliane Weber for critically reading the manuscript. This study was supported by the RTK 2155 (ProMoAge).

DISCLOSURES:

The authors have nothing to disclose.

REFERENCES:

1. Goldmann, E. E. Vitalfärbung am Zentralnervensystem: Beitrag z. Physio-Pathologie d. Plexus chorioideus und Hirnhäute. (1913).
2. Reese, T. S., Karnovsky, M. J. Fine structural localization of a blood-brain barrier to exogenous peroxidase. *Journal of Cell Biology*. 34 (1), 207–217 (1967).
3. Risau, W., Dingler, A., Albrecht, U., Dehouck, M. P., Cecchelli, R. Blood-brain barrier pericytes are the main source of gamma-glutamyltranspeptidase activity in brain capillaries. *Journal of Neurochemistry*. 58 (2), 667–672 (1992).
4. Brightman, M. W., Reese, T. S. Junctions between intimately apposed cell membranes in the vertebrate brain. *Journal of Cell Biology*. 40 (3), 648–677 (1969).
5. Coomber, B. L., Stewart, P. A. Morphometric analysis of CNS microvascular endothelium. *Microvascular Research*. 30 (1), 99–115 (1985).

6. Tilling, T., Korte, D., Hoheisel, D., Galla, H. J. Basement membrane proteins influence brain capillary endothelial barrier function in vitro. *Journal of Neurochemistry*. 71 (3), 1151–1157 (1998).
7. Morris, A. W. et al. Vascular basement membranes as pathways for the passage of fluid into and out of the brain. *Acta Neuropathologica*. 131 (5), 725–736 (2016).
8. Betz, A. L., Goldstein, G. W. Polarity of the blood-brain barrier: neutral amino acid transport into isolated brain capillaries. *Science*. 202 (4364), 225–227 (1978).
9. Butt, A. M., Jones H. C., Abbott N. J. Electrical resistance across the blood-brain barrier in anaesthetized rats: a developmental study. *Journal of Physiology*. 429, 47–62 (1990).
10. Calabria, A. R., Weidenfeller, C., Jones, A. R., de Vries, H. E., Shusta, E. V. Puromycin-purified rat brain microvascular endothelial cell cultures exhibit improved barrier properties in response to glucocorticoid induction. *Journal of Neurochemistry*. 97 (4), 922–933 (2006).
11. O'Carroll, S. J. et al. Pro-inflammatory TNF α and IL-1 β differentially regulate the inflammatory phenotype of brain microvascular endothelial cells. *Journal of Neuroinflammation*. 12 (131) (2015).
12. Simi, A., Tsakiri, N., Wang, P., Rothwell, N. J. Interleukin-1 and inflammatory neurodegeneration. *Biochemical Society Transactions*. 35 (Pt 5), 1122–1126 (2007).
13. Janzer, R. C., Raff, M. C. Astrocytes induce blood-brain barrier properties in endothelial cells. *Nature*. 325 (6101), 253–257 (1987).
14. Tao-Cheng, J. H., Nagy, Z., Brightman, M. W. Tight junctions of brain endothelium in vitro are enhanced by astroglia. *Journal of Neuroscience*. 7 (10), 3293–3299 (1987).
15. Utsumi, H. et al. Expression of GFR α -1, receptor for GDNF, in rat brain capillary during postnatal development of the BBB. *American Journal of Physiology and Cell Physiology*. 279 (2) (2000).
16. Tran, N. D., Correale, J., Schreiber, S. S., Fisher, M. Transforming growth factor-beta mediates astrocyte-specific regulation of brain endothelial anticoagulant factors. *Stroke*. 30 (8), 1671–1678 (1999).
17. Balabanov, R., Washington, R., Wagnerova, J., Dore-Duffy, P. CNS microvascular pericytes express macrophage-like function, cell surface integrin α M, and macrophage marker ED-2. *Microvascular Research*. 52 (2), 127–142 (1996).

18. Ramsauer, M., Krause, D., Dermietzel, R. Angiogenesis of the blood-brain barrier in vitro and the function of cerebral pericytes. *Faseb Journal*. 16 (10), 1274–1276 (2002).
19. Lindahl, P., Johansson, B. R., Leveen, P., Betsholtz, C. Pericyte loss and microaneurysm formation in PDGF-B-deficient mice. *Science*. 277 (5323), 242–245 (1997).
20. Young, G. B., Bolton, C. F., Archibald, Y. M., Austin, T. W., Wells, G. A. The electroencephalogram in sepsis-associated encephalopathy. *Journal of Clinical Neurophysiology*. 9 (1), 145–152 (1992).
21. Carlyle Clawson, C., Francis Hartmann, J., Vernier, R. L. Electron microscopy of the effect of gram-negative endotoxin on the blood-brain barrier. *Journal of Comparative Neurology*. 127 (2), 183–197 (1966).
22. Jeppsson, B. et al. Blood-brain barrier derangement in sepsis: cause of septic encephalopathy? *The American Journal of Surgery*. 141 (1), 136–142 (1981).
23. Tighe, D., Moss, R., Bennett, D. Cell surface adrenergic receptor stimulation modifies the endothelial response to SIRS. *Systemic Inflammatory Response Syndrome*. *New Horizons* (Baltimore, Md.). 4 (4), 426–442 (1996).
24. Kim, K. S. et al. The K1 capsule is the critical determinant in the development of *Escherichia coli* meningitis in the rat. *Journal of Clinical Investigation*. 90 (3), 897–905 (1992).
25. Kim, K. S., Wass, C. A., Cross, A. S. Blood-brain barrier permeability during the development of experimental bacterial meningitis in the rat. *Experimental Neurology*. 145 (1), 253–257 (1997).
26. Arshi, A. et al. Predictors and Sequelae of Postoperative Delirium in Geriatric Hip Fracture Patients. *Geriatric Orthopaedic Surgery and Rehabilitation*. 9, 2151459318814823 (2018).
27. Smulter, N., Lingehall, H. C., Gustafson, Y., Olofsson, B., Engstrom, K. G. Delirium after cardiac surgery: incidence and risk factors. *Interactive CardioVascular and Thoracic Surgery*. 17 (5) (2013).
28. Kratz, T., Heinrich, M., Schlauss, E., Diefenbacher, A. Preventing postoperative delirium. *Deutsches Arzteblatt International*. 112 (17), 289–296 (2015).
29. Uchida, Y. et al. Quantitative targeted absolute proteomics of human blood-brain barrier transporters and receptors. *Journal of Neurochemistry*. 117 (2), 333–345 (2011).

30. Warren, M. S. et al. Comparative gene expression profiles of ABC transporters in brain microvessel endothelial cells and brain in five species including human. *Pharmacology Research*. 59 (6), 404–413 (2009).
31. Omid, Y. et al. Evaluation of the immortalised mouse brain capillary endothelial cell line, b.End3, as an in vitro blood-brain barrier model for drug uptake and transport studies. *Brain Research*. 990 (1–2), 95–112 (2003).
32. Steiner, O., Coisne, C., Engelhardt, B., Lyck, R. Comparison of immortalized bEnd5 and primary mouse brain microvascular endothelial cells as in vitro blood-brain barrier models for the study of T cell extravasation. *Journal of Cerebral Blood Flow and Metabolism*. 31 (1), 315–327 (2011).
33. Burek, M., Salvador, E., Forster, C. Y. Generation of an immortalized murine brain microvascular endothelial cell line as an in vitro blood brain barrier model. *Journal of Visualized Experiment*. (66), e4022 (2012).
34. Ohtsuki, S. et al. Quantitative targeted absolute proteomic analysis of transporters, receptors and junction proteins for validation of human cerebral microvascular endothelial cell line hCMEC/D3 as a human blood-brain barrier model. *Molecular Pharmacology*. 10 (1), 289–296 (2013).
35. Urich, E., Lazic, S. E., Molnos, J., Wells, I., Freskgard, P. O. Transcriptional profiling of human brain endothelial cells reveals key properties crucial for predictive in vitro blood-brain barrier models. *PLoS One*. 7 (5), e38149 (2012).
36. Lopez-Ramirez, M. A. et al. Cytokine-induced changes in the gene expression profile of a human cerebral microvascular endothelial cell-line, hCMEC/D3. *Fluid Barrier CNS*. 10 (27) (2013).
37. Cucullo, L. et al. Immortalized human brain endothelial cells and flow-based vascular modeling: a marriage of convenience for rational neurovascular studies. *Journal of Cerebral Blood Flow Metabolism*. 28 (2), 312–328 (2008).
38. Lippmann, E. S. et al. Derivation of blood-brain barrier endothelial cells from human pluripotent stem cells. *Nature Biotechnology*. 30 (8), 783–791 (2012).
39. Boyer-Di Ponio, J. et al. Instruction of circulating endothelial progenitors in vitro towards specialized blood-brain barrier and arterial phenotypes. *PLoS One*. 9 (1), e84179 (2014).
40. Cecchelli, R. et al. A stable and reproducible human blood-brain barrier model derived from hematopoietic stem cells. *PLoS One*. 9 (6), e99733 (2014).
41. Lippmann, E. S., Al-Ahmad, A., Azarin, S. M., Palecek, S. P., Shusta, E. V. A retinoic acid-enhanced, multicellular human blood-brain barrier model derived from stem cell sources. *Science Reports*. 4, 4160 (2014).

42. Lim, R. G. et al. Huntington's Disease iPSC-Derived Brain Microvascular Endothelial Cells Reveal WNT-Mediated Angiogenic and Blood-Brain Barrier Deficits. *Cell Reports*. 19 (7), 1365–1377 (2017).
43. Stins, M. F., Badger, J., Sik Kim, K. Bacterial invasion and transcytosis in transfected human brain microvascular endothelial cells. *Microbiological Pathogens*. 30 (1), 19–28 (2001).
44. Gaschignard, J. et al. Neonatal Bacterial Meningitis: 444 Cases in 7 Years. *Pediatric Infectious Disease Journal*. 30 (3), 212–217 (2011).
45. Hussain, M. The Effect of Glycation on the Permeability of an in vitro Blood--brain Barrier Model, University Halle - Wittenberg (2015).
46. Weber, V. The effect of glycation on the permeability of human blood-brain barrier (University Halle-Wittenberg, 2019).
47. Hussain, M. et al. Novel insights in the dysfunction of human blood-brain barrier after glycation. *Mechanism of Ageing Development*. 155, 48–54 (2016).
48. Choi, C. Bacterial meningitis in aging adults. *Clinical Infectious Disease*. 33 (8), 1380–1385 (2001).
49. Furth, A. J. Glycated proteins in diabetes. *British Journal of Biomedical Science*. 54 (3), 192–200 (1997).
50. Sajithlal, G. B., Chithra, P., Chandrakasan, G. Advanced glycation end products induce crosslinking of collagen in vitro. *Biochimica and Biophysica Acta*. 1407 (3), 215–224 (1998).
51. Ray, R., Juranek, J. K., Rai, V. RAGE axis in neuroinflammation, neurodegeneration and its emerging role in the pathogenesis of amyotrophic lateral sclerosis. *Neuroscience and Biobehavior Reviews*. 62, 48–55 (2016).
52. DeBault, L. E., Cancilla, P. A. Gamma-Glutamyl transpeptidase in isolated brain endothelial cells: induction by glial cells in vitro. *Science*. 207 (4431), 653–655 (1980).
53. Diglio, C. A., Grammas, P., Giacomelli, F., Wiener, J. Primary culture of rat cerebral microvascular endothelial cells. Isolation, growth, and characterization. *Laboratory Investigation*. 46 (6), 554–563 (1982).
54. Buchert, M., Turksen, K., Hollande, F. Methods to examine tight junction physiology in cancer stem cells: TEER, paracellular permeability, and dilution potential measurements. *Stem Cell Reviews*. 8 (3), 1030–1034 (2012).

55. Gibson, B., Wilson, D. J., Feil, E., Eyre-Walker, A. The distribution of bacterial doubling times in the wild. *Proceedings of the Royal Society B: Biological Sciences*. 285 (1880) (2018).
56. Pron, B. et al. Interaction of *Neisseria meningitidis* with the components of the blood-brain barrier correlates with an increased expression of PilC. *Journal of Infectious Diseases*. 176 (5), 1285–1292 (1997).
57. Iovino, F., Orihuela, C. J., Moorlag, H. E., Molema, G., Bijlsma, J. J. Interactions between blood-borne *Streptococcus pneumoniae* and the blood-brain barrier preceding meningitis. *PLoS One*. 8 (7), e68408 (2013).

Glycation Increases the Risk of Microbial Traversal through an Endothelial Model of the Human Blood-Brain Barrier after Use of Anesthetics

Veronika Weber ^{1,†}, Heidi Olzscha ^{1,*†}, Timo Längrich ¹, Carla Hartmann ², Matthias Jung ², Britt Hofmann ³, Rüdiger Horstkorte ¹ and Kaya Bork ¹

¹ Institut für Physiologische Chemie, Martin-Luther-Universität Halle-Wittenberg, Hollystr. 1, 06114 Halle (Saale), Germany

² Klinik und Poliklinik für Psychiatrie, Psychotherapie und Psychosomatik, Martin-Luther-Universität Halle-Wittenberg, Julius-Kühn-Str. 7, 06112 Halle (Saale), Germany

³ Klinik und Poliklinik für Herzchirurgie, Universitätsklinikum Halle (Saale), Ernst-Grube-Str. 20, 06120 Halle (Saale), Germany

* Author to whom correspondence should be addressed.

† These authors contributed equally.

J. Clin. Med. **2020**, *9*(11), 3672; <https://doi.org/10.3390/jcm9113672>

Received: 8 October 2020 / Revised: 10 November 2020 / Accepted: 11 November 2020 / Published: 16 November 2020

Abstract: The function of the human blood–brain barrier (BBB), consisting mainly of the basement membrane and microvascular endothelial cells, is to protect the brain and regulate its metabolism. Dysfunction of the BBB can lead to increased permeability, which can be linked with several pathologies, including meningitis, sepsis, and postoperative delirium. Advanced glycation end products (AGE) are non-enzymatic, posttranslational modifications of proteins, which can affect their function. Increased AGE levels are strongly associated with ageing and degenerative diseases including diabetes. Several studies demonstrated that the formation of AGE interfere with the function of the BBB and may change its permeability for soluble compounds. However, it is still unclear whether AGE can facilitate microbial traversal through the BBB and how small compounds including anesthetics modulate this process. Therefore, we developed a cellular model, which allows for the convenient testing of different factors and compounds with a direct correlation to bacterial traversal through the BBB. Our results demonstrate that both glycation and anesthetics interfere with the

function of the BBB and promote microbial traversal. Importantly, we also show that the essential nutrient and antioxidant ascorbic acid, commonly known as vitamin C, can reduce the microbial traversal through the BBB and partly reverse the effects of AGE.

Keywords: Advanced glycation endproducts (AGE); anesthetics; ascorbic acid; blood–brain barrier; diabetes mellitus; glycation; human brain microvascular endothelial cells; meningitis; microbial traversal; propofol

1. Introduction

Due to the increased life span, age-related diseases, and consecutive demographic changes, health and mental performance in the elderly is becoming more important. The involvement of advanced glycation end products (AGE) is one possible cause for molecular ageing and correlates with the development of age-related diseases, in particular diabetes [1]. During normal ageing, AGE accumulate in the organism, thus contributing to the molecular mechanisms of cellular ageing [2,3]. AGE are built during glycation, a non-enzymatically condensation reaction between the carbonyl group of reducing carbohydrates or metabolites and free amino groups. The reaction includes the reversible formation of Schiff bases, which further rearrange to so-called Amadori products, and which are finally converted to AGE [4]. Histopathologic studies already showed accumulations of a diversity of AGE in the lung, liver, kidney, or amyloid plaques in Alzheimer's disease [5]. Fragmentation of Amadori products can result in the formation of methylglyoxal (MGO), which is also formed as a regular by-product of glycolysis. Up to 0.4% of all glucose molecules are metabolized to MGO per cycle of glycolysis, whereby concentrations can be even higher in impaired glucose utilization or hyperglycemia [6,7]. MGO is a highly reactive dicarbonyl molecule, leading to the formation of different AGE. In general, the accumulation of dicarbonyl components is also referred to as carbonyl stress [2,8]. The pathology of AGE is mediated through different mechanisms. The generation of protein modifications or cross-links of extra- or intracellular components can alter protein function or even results in a complete loss of protein function [1]. Another aspect to be mentioned is the binding of AGE to receptors, such as the receptor for advanced glycation end products (RAGE), thereby activating pro-inflammatory signal transduction cascades [8]. Endothelial cells cultivated in high glucose concentrations show an increased RAGE activity which leads to increased endothelial cell permeability [9].

Since AGE can basically affect all proteins, they also interfere with proteins of the blood-brain barrier (BBB). The BBB is a tight barrier which separates the blood from the brain, regulates the access of large and hydrophilic molecules to the brain and ensures that the brain can act in a metabolically strictly controlled compartment [10]. The most important cell type forming the tight BBB are the brain microvascular endothelial cells (BMECs). They have some unique features which distinguish them from other endothelial cells, such as a high number of tight junctions and adherens junctions [11] and a continuous basement membrane [12]. There are certain marker proteins for the tight junctions between the BMECs, e.g., occludin, whose level are high in intact BMECs [13]. Another marker protein in BMECs is VE-cadherin, a transmembrane protein which mainly constitutes the adherens junctions and is linked to the actin cytoskeleton with catenins [14]. Many diseases are associated with increased permeability of the BBB, including bacterial meningitis and sepsis [15]. Additionally, iatrogenic disorders can be accompanied with a more permeable BBB, an example would be the postoperative delirium, which is strongly associated with preoperative infections [16,17] and diabetes has been found as independent predisposing factor [18].

Multiple studies have shown that patients with diabetes have a two-fold higher risk of developing meningitis or encephalitis with hyperglycemia remaining a risk factor for severe outcomes and increase of mortality [19–21]. In addition to the immunosuppressing effects of diabetes, there are indications that AGE can be causative for an increased permeability of the BBB and some mechanistic aspects give further evidence for this hypothesis. For instance, Shimizu et al. showed in a study that AGE reduced the expression of claudin 5 in BMECs by increasing autocrine signaling via the vascular endothelial growth factor (VEGF) cascade. They also proposed that AGE increase the degree of autocrine TGF- β signaling by pericytes, and thereby weaken the BBB through the up-regulation of VEGF and MMP-2 in BMECs under diabetic conditions [22]. The expression of the proteins zonula occludens-1 (ZO-1) and occludin is downregulated by MGO in a model built with THBMEC [23]. Another study revealed that AGE can cause phosphorylation of myosin in murine brain microvascular endothelial cells with p38 and Rho kinase pathway activation [24]. Kim et al. showed that the primary entry site of circulating bacteria is the microvessels [25]. However, the BBB prevents the entry of bacteria. The ability of bacteria entering the brain via transcellular as well as paracellular traversal is related to the interaction with proteins which are also affected by AGE, such as VEGF [26,27], ZO-1, or occludin [28].

However, it has not been clarified, so far, how and to what degree AGE can cause an increased permeability of the BBB that even bacteria could traverse easier through the barrier, leading to the mentioned disease of bacterial meningitis. It has also not been systematically evaluated, how compounds affecting the brain, especially anesthetics, can influence the permeability of the BBB. There are studies showing that propofol as a common anesthetic induce cellular stress and support the breakdown of BBB [29,30]. In addition, some studies proof the neuroprotective effect of propofol by tighten the BBB and lower incidence of post-operative delirium compared with other anesthetics such as sevoflurane [31,32].

In this study, we report the usage of a newly developed BBB model system [33] to analyze the effects of AGE on the permeability of the BBB, how this can modulate a propofol response and how bacterial traversal would be affected. We could demonstrate that bacterial traversal increases upon treatment of the cells with physiological doses of an AGE building compound. We also could show that anesthetics such as propofol and supplements in anesthesia including norepinephrine lead to an increase of the BBB permeability for bacteria. Importantly, the antioxidant ascorbic acid, more commonly known as vitamin C, can partly reverse the effects of the AGE building compound, propofol and norepinephrine. Similarly, it has been shown that ascorbic acid has positive effects on the permeability of glycated blood-brain barrier cells measured by transendothelial inulin transfer [9]. We propose that ascorbic acid can be beneficial in reducing the effects of diabetic encephalopathy which is accepted as an important complication of diabetes and preventing adverse effects on the BBB during anesthesia.

2. Experimental Section

2.1. Cells and Cell Culture

Transfected human brain microvascular endothelial cells (THBMEC) [34] were kindly provided by the group of MF Stins (Los Angeles, CA, USA). Cells were cultivated in DMEM F12 medium (Thermo Fisher Scientific, Waltham, MA, USA) at 37 °C in a humidified cell culture incubator. Supplemented medium was prepared by adding 100 mg/L penicillin and 100 mg/L streptomycin (Thermo Fisher Scientific), 2 mM L-glutamine (Thermo Fisher Scientific) and 4% heat-inactivated fetal calf serum (GE Healthcare, Little Chalfont, UK). Cells were passaged every 3–4 days. THBMECs were detached with Trypsin/EDTA (Thermo Fisher Scientific) and pelleted at 210 g for 3 min. Further particulars can be found in [33].

2.2. Treatment for Immunoblotting

For the immunoblots showing glycation of cells, THMBECs were incubated in medium supplemented with methylglyoxal (MGO) (Sigma Aldrich, St. Louis, USA) for 1 h. Different concentrations, i.e., 0.05 mM, 0.15 mM, 0.45 mM, or 1 mM, of MGO were used for immunoblotting. Additionally, an immunoblot for detection of CD31 was performed. Therefore, cells were incubated with medium supplemented with interleukin 1 β (IL1 β) (Immunotools, Friesoythe, GER) and tumor necrosis factor α (TNF α) (Immunotools) for 24 h. A concentration of 0.05 ng/mL was used. Cells were incubated in a humidified incubator at 37 °C. Untreated THBMECs cultured in media served as a control.

2.3. Preparation of Cell Extracts

After incubation, treated and control cells were washed twice with PBS. Cells were removed from the surface by scraping and directly lysed into SDS-sample buffer (100 mL buffer containing 12.5% SDS, 0.3 M Tris, 50 mL glycerin, bromophenol blue at pH 6.8 and 1:10 DTT to buffer) which was pre-warmed for 5 min by 90 °C. After mixing, the cell extracts were used for downstream analysis.

2.4. Immunoblotting

Proteins of the samples were separated by SDS-PAGE on a 10% acrylamide gel and transferred afterwards to a nitrocellulose membrane for 1 h 15 min in blotting buffer with a constant amperage of 25 mA per gel. During the blotting process, the blot chamber (VWR, Radnor, USA) was cooled down to avoid overheating. The following staining with ponceau red solution containing 0.1% ponceau S (Carl Roth, Karlsruhe, Germany), 3% trichloroacetic acid and 3% sulfosalicylic acid proved a successful protein transfer on to the membrane. The membrane was washed twice with water and was then blocked for 1 h at room temperature using 5% milk in TBS. The membrane was then incubated with the primary antibodies overnight at 4 °C. Glycation was detected by the monoclonal antibody CML-26 (ab12514, Abcam, Cambridge, CB2 0AX, UK) at a 1:10,000 dilution. CD31 was detected using the monoclonal anti-CD31-Antibody (ab24590, Abcam) at a dilution of 1:1000. VE-cadherin was detected by a monoclonal antibody (ab166715, Abcam), diluted 1:1000. Occludin was detected using anti-occludin-Antibody (ab167161, Abcam) at a 1:100,000 dilution. To detect integrin- β 1, the membrane was blocked for 1 h at room temperature using 5 % bovine serum albumin (BSA) (Carl Roth) in TBS. Afterwards, the membrane was incubated with anti-

integrin- β 1-antibody (Cell Signaling Technology, Frankfurt a. M., Germany diluted 1:1000 in BSA. After incubation with primary antibody, the membrane was washed three times with 1 x PBS for 10 min and incubated with the corresponding peroxidase-conjugated secondary antibody. Therefore, a monoclonal mouse-antibody (ab6789, Abcam) diluted 1:10,000 or rabbit-antibody (ab6721, Abcam) diluted 1:20,000 were used. The proteins were detected using Luminata Forte Western HRP-Substrate (Merck Millipore, Billerica, MA, USA) and signals were visualized using the ChemiDoc MP Imaging System (BioRad, Hercules, CA, USA). Occurring bands were analyzed using the associated ImageLab software (BioRad). Ponceau S staining served as loading control and was used to normalize the band intensity of the Western blot. The total protein normalization was recommended by the software producer as a better alternative to housekeeping protein normalization.

2.5. MTT-Assay

MTT assays were performed to determine the cytotoxicity of different cell treatments by measuring the metabolic activity. THBMECs were seeded into 96-well microtiter plates at a density of 1×10^5 per well and treated with 0.15 mM MGO for 1 h, 3 μ g/mL propofol (propofol 2%, Fresenius Kabi, SGP) for 3 h or 1 ng/mL norepinephrine (Arterenol® 1 mg/mL, Sanofi-Aventis, Frankfurt a.M., GER) for 1 h added to medium. After treatment cells were washed with 200 μ L PBS per well. MTT (Sigma, Saint Louis, MI, USA) was diluted to a concentration of 0.5 mg/mL in normal medium and 100 μ L were added to each well and incubated for 4 h in a humidified incubator. After removal of MTT containing medium, remaining formazan crystals were dissolved in 150 μ L DMSO (Sigma, Saint Louis, MI, USA). The absorbance was measured photometrically at a wavelength of 570 nm (background 630 nm) on a microplate reader Multiskan EX (Thermo Fisher Scientific, Rockford, USA). Relative cell viability was calculated and compared to the untreated control, which were set to 100% of metabolic activity.

2.6. Measurement of Bacterial Traversal through the BBB

To test the effect of different compounds on the permeability of the human BBB, we developed an endothelial cell culture model, which mimics a tight BBB model with THBMECs. Cells were treated and exposed to bacteria as previously described [33]. In brief, THBMECs were grown on 12-well filters with 3.0- μ m pore size (ThinCerts, Greiner Bio-One, Austria) to a confluent layer. Before seeding cells, filters were coated with 10 μ g/mL collagen IV and 10 μ g/mL fibronectin (Sigma, Saint Louis, USA) mixture

for 24 h. The cells were incubated for 14 days in a cell culture incubator with 5% CO₂ atmosphere at 37 °C, changing the DMEM/F12 medium every 2 to 3 days in the upper and lower chamber. Afterwards, they were treated with the different compounds. In the next step, medium from both chambers was changed to antibiotic free DMEM/F12 medium and E.coli strain GM2163 (Fermentas Life Sciences, Lithuania) bacteria were then fed into the upper chamber. After 6 h, samples from the lower chamber were plated and colonies were counted.

2.7. Treatment for Measurement of Bacterial Traversal through the BBB

To treat the cell monolayer in our model, THBMECs were grown for 14 days to confluence which were proofed by evaluating cell density on the filters with a microscope. Exemplarily, we measured the transendothelial electrical resistance (TEER) of 70 $\Omega \cdot \text{cm}^2$ after growing on filters for 14 days (Supplementary Figure S1). Afterwards, THBMECS were incubated in medium supplemented with different compounds. To test the effect of glycation, cells were washed with PBS and medium supplemented with 0.15 mM MGO was given into the upper and lower chamber for 1 h. To test the effect of anesthetics, cells were washed with PBS and medium where 3 $\mu\text{g}/\text{mL}$ propofol for 3 h or 1 ng/mL norepinephrine were given into both chambers for 1 h. Incubation in medium supplemented with Intralipid (SMO Flipid 200 mg/mL, Fresenius Kabi) for 3 h and sodium metabisulfite for 1 h (PanReacAppliChem, ITW Reagents, Darmstadt, GER) served as control. To test the effect of vitamin C, cells were incubated with 0.1 mM ascorbic acid (AA) (Carl Roth) for 4 h added to medium in both chambers. Additionally, cells were first incubated with medium supplemented with 0.15 mM MGO and afterwards they were washed with PBS and medium supplemented with 0.1 mM AA were added. In addition, the reverse procedure was performed with AA treatment first followed by treatment with MGO. Untreated cells served as control.

2.8. RNA Extraction and Barrier Genes High-Throughput Multiplex qPCR

RNA was isolated using the NucleoSpinTM RNA kit according to manufacturer's protocol (Macherey-Nagel, Cat. No. 740955.250) from the indicated cell lines. Samples of 250 ng RNA were transcribed to cDNA using the High-Capacity cDNA Reverse 191 Transcription Kit (Applied Biosystems, Cat. No. 4368814), according to the manufacturer's instructions. Targets were preamplified using tenfold concentrated primer pools, mastermix, and the following program: 15 min at 95 °C for HotStar Plus Taq Polymerase (Qiagen, Cat. No. 203603), 18 cycles of 40 s at 95 °C, 40 s at 60 °C, 80 s at 72 °C, and 7 min at 72 °C. We used a BiomarkTM system containing an IFC

Controller HX and 96.96 Dynamic ArraysTM IFC, according to the manufacturer's instructions. In brief, each sample well was loaded with TagmanTM gene expression mastermix, DNA binding dye sample loading reagent, EvaGreenTM binding dye, and 1:8 diluted preamplified cDNA. Target wells were loaded with assay loading reagent and the respective primers. After qPCR and data allocation, the Ct values of the targets were normalized to the endogenous control B2M. The Δ Ct values were used for the following statistical analysis applying the software Graph Pad Prism 7 (GraphPad, San Diego, CA, USA).

2.9. Statistical Analysis

Data are represented as bar diagrams or data points including mean \pm standard error of measurement (SEM). Statistical analyses were performed using OriginPro2017 software (OriginLab Corporation, Northampton, MA, USA) or Graph Pad Prism 7 (GraphPad, San Diego, CA, USA). Unpaired student t-test against the control group or a theoretical value of 1 (due to data normalization) was used for microbial traversal after treatment with MGO. ANOVA and Tukey Kramer as post hoc tests were used for every other data. A difference between untreated and treated samples at $p < 0.05$ was considered as statistically significant, and significant p-values are displayed on each graph. RNA extraction and barrier genes high-throughput multiplex qPCR has been performed in two technical replicates for each cell line.

3. Results

In order to analyze the effects of glycation and anesthetics on bacterial traversal through the BBB, a model, which mimics the BBB, was built-up by human brain endothelial cells (THBMEC) [33,34]. These cells were grown on filters until confluence to prevent bacteria in the upper chamber from crossing into the lower chamber. Since this barrier is built-up by cell junctions of THBMECs, we firstly characterized the expression of common tight and adherens junction proteins at the beginning and end of the two weeks of cell cultivation.

3.1. Determination of Protein Levels Building the Cell Junctions

Occludin is an important protein of tight junctions, therefore we decided to analyze their levels by immunoblotting. There was a significant increase of occludin expression between day 2 and 16 (Figure 1a). VE-cadherin as a representative protein of adherens junctions increased between day 2 and 16 as well (Figure 1b). Integrin- β 1 did not display increased expression over time (Figure 1c), but was also an important

protein for cell adherence and cell signaling. We also treated the cells for 24 h with interleukin-1-beta (IL1 β) and tumor necrosis factor alpha (TNF α) to analyze, whether THBMECs were able to react on proinflammatory mediators. A marker for this event was the platelet endothelial cell adherence molecule (PECAM or CD31), which primarily regulates leukocyte transmigration. The expression of CD31 increased regardless of whether using concentrations of 0.05 ng/mL or 10 ng/mL of IL1 β or TNF α (Figure 1d), as proven by immunoblotting. The presence of mRNA coding for various other proteins with crucial functions in building tight junctions could be confirmed by qPCR in the THBMECs compared to hCMECs/D3 cells (Supplementary Figure S2).

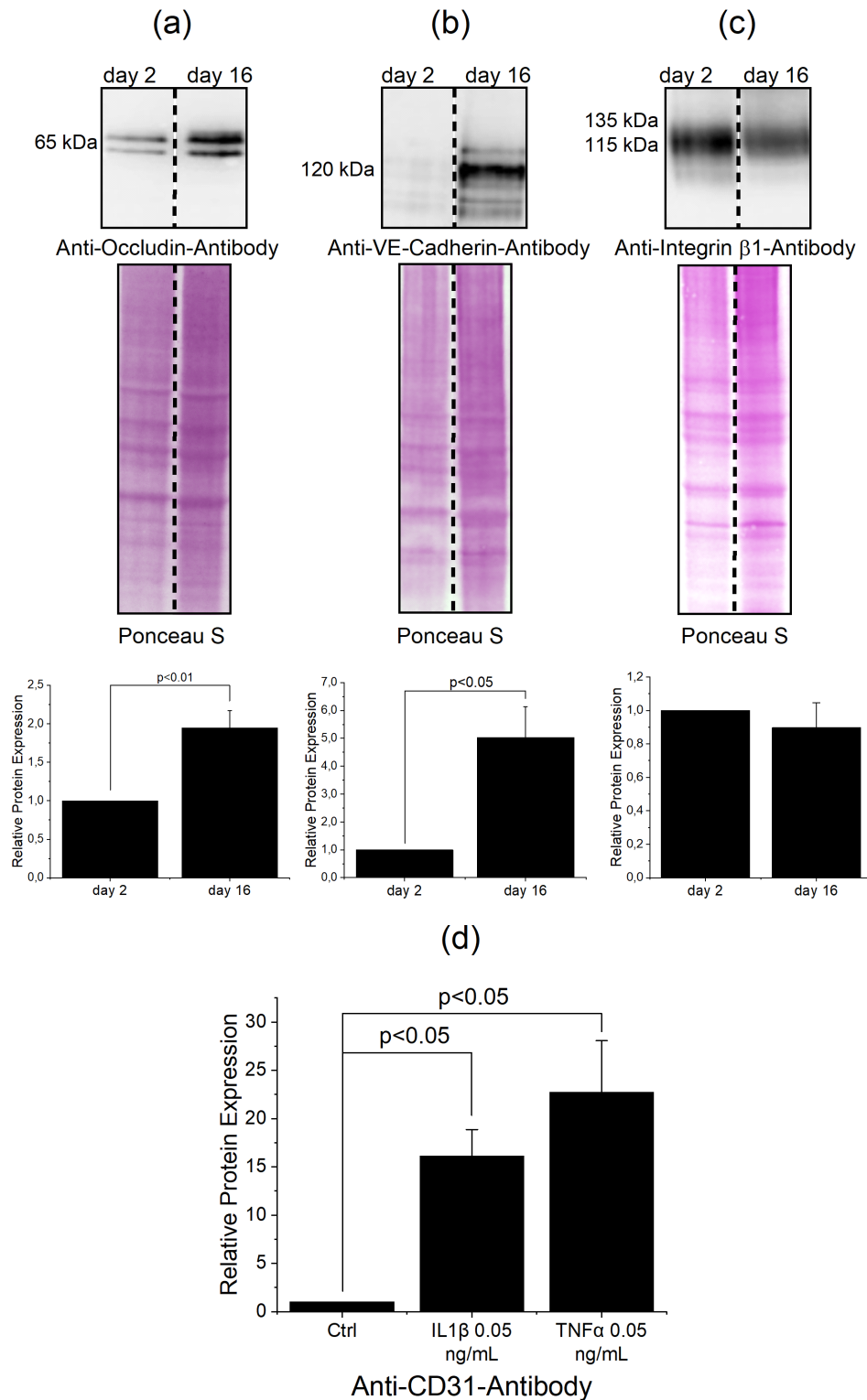


Figure 1. Determination of protein levels building the cell junctions in THBMECs. THBMECs were cultivated for 2 and 16 days. Afterwards, total protein was isolated and separated using SDS-PAGE. Expression of proteins was detected via immuno-blotting using anti-occludin antibody (a), anti-VE-cadherin antibody (b) and anti-integrin β 1 antibody (c), respectively (n = 3). THBMECs were incubated with IL1 β and TNF α at a

concentration of 0.05 ng/mL for 24 h. Total protein was isolated and separated using SDS-PAGE. Expression of CD31 was detected by immuno-blotting using anti-CD31 antibody (d), (n = 3).

3.2. Protein Glycation is Induced by MGO

To analyze the effect of glycation on cells, we treated them with MGO to induce formation of AGE. The treatment lasted 1 h and different concentrations of MGO were used to find the lowest AGE inducing concentration for further experiments. AGE were detected by immunoblotting after treatment with 0.05 mM, 0.15 mM, 0.45 mM, or 1 mM MGO (Figure 2a). The immunoblots were quantitated (Figure 2b). According to the results, we decided to use 0.15 mM MGO for 1 h in all our further experiments, since these concentrations have been measured in patients [35]. Additionally, cell viability assays were performed to assess the treatment of cells with 0.15 mM MGO for 1 h. The assay did not show toxic effects of 0.15 mM MGO treatment for 1 h on THBMECs or interference with cellular proliferation (Figure 2d). Untreated cells served as control in this assay. We also tested whether the expression levels of RAGE change during the treatment and whether the Western blot signal would be masked by AGE. We could detect RAGE in the THBMECs by immunoblotting with or without treatment of MGO, whereby the protein level did not change after an hour of treatment with MGO (Supplementary Figure S3).

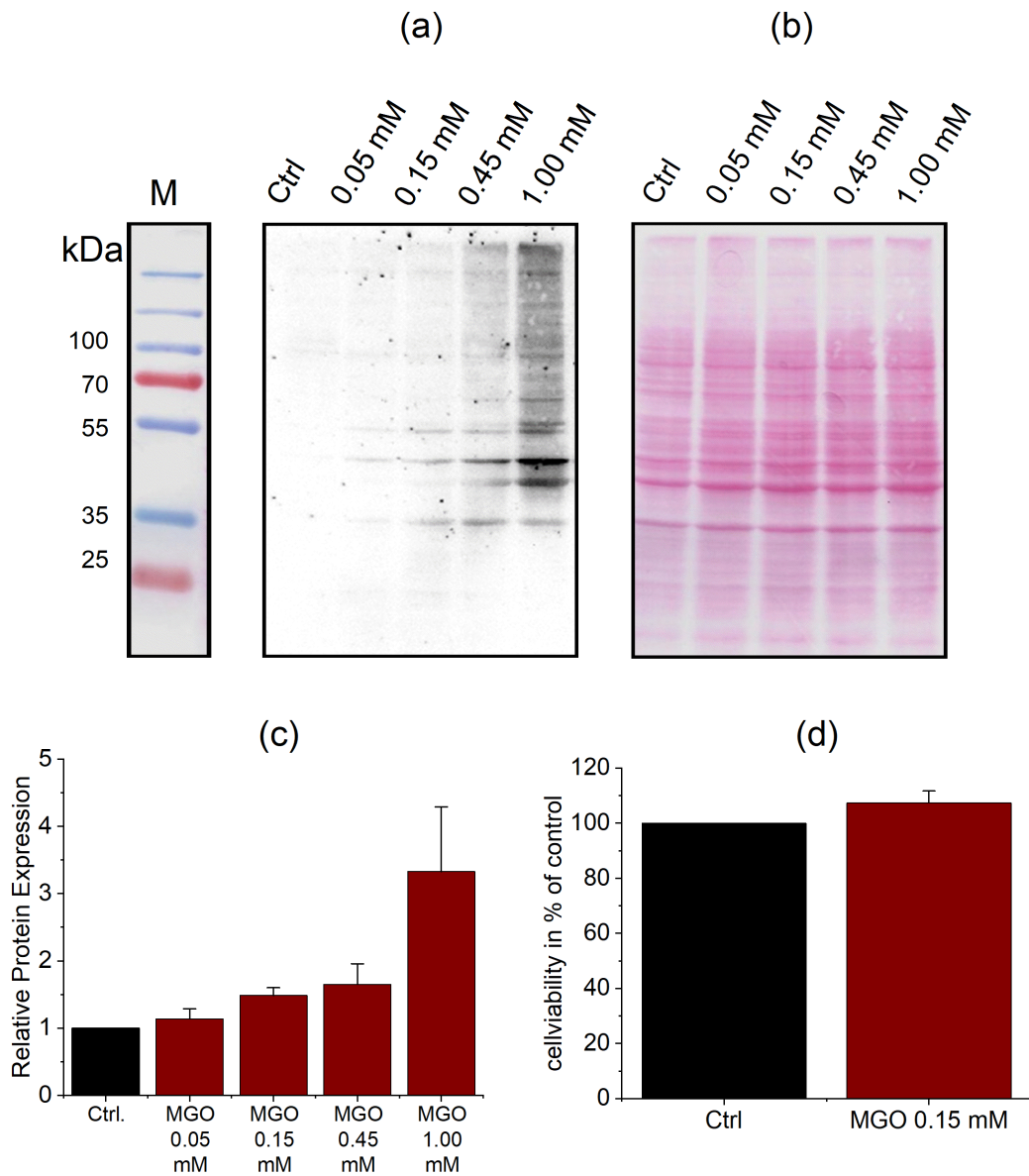


Figure 2. THBMECs were incubated with MGO at different concentrations for 1 h in normal medium. Total protein was isolated and separated using SDS-PAGE. Glycation of proteins was detected by immuno-blotting using anti-AGE-antibody (CML-26) (a). Ponceau S staining served as loading control (b). The bar graph shows the mean + SEM of relative protein glycation detected by immunoblotting, untreated cells serve as control (c), (n = 5). Cell viability in THBMECs upon treatment with MGO (d). Cells were treated with 0.15 mM MGO for 1 h. Afterwards, MTT assays were performed. The graph shows the mean + SEM of the absorbance of formazan crystals at a wavelength of 570 nm, untreated cells served as control, (n = 3).

3.3. Protein Glycation Increases the Permeability of the BBB, Which Can Be Reverted by Antioxidant

In order to analyze the effect of glycation on bacterial traversal, we built the model of human BBB with THBMECs and after cultivation of 14 days, cells were treated with 0.15 mM MGO for 1 h. The upper chamber was then inoculated with bacteria and, after 6 h, medium from the lower chamber was plated and colonies were counted. Untreated cells served as control and showed a low bacterial traversal with 6.2 colonies on average. Compared to this 0.15 mM MGO for 1 h affected the traversal by increasing the number of colonies up to 47 colonies on average (Figure 3). In addition, we wanted to test some compounds with anti-glycation effects in our model of the human blood-brain barrier. An agent we took into consideration fulfilling the requirement was ascorbic acid (AA), better known as vitamin C. It is a reducing agent, but in addition, it provided the risk of glycation by itself [36]. We used 0.1 mM ascorbic acid for 4 h and MGO with 0.15 mM for 1 h to treat cells after 14 d of cultivation. Additionally, we combined both treatments—first ascorbic acid then MGO or vice versa. The glycated cells with the additional ascorbic acid treatment showed a significant decrease of microbial traversal compared to cells, which were only treated with MGO (Figure 3).

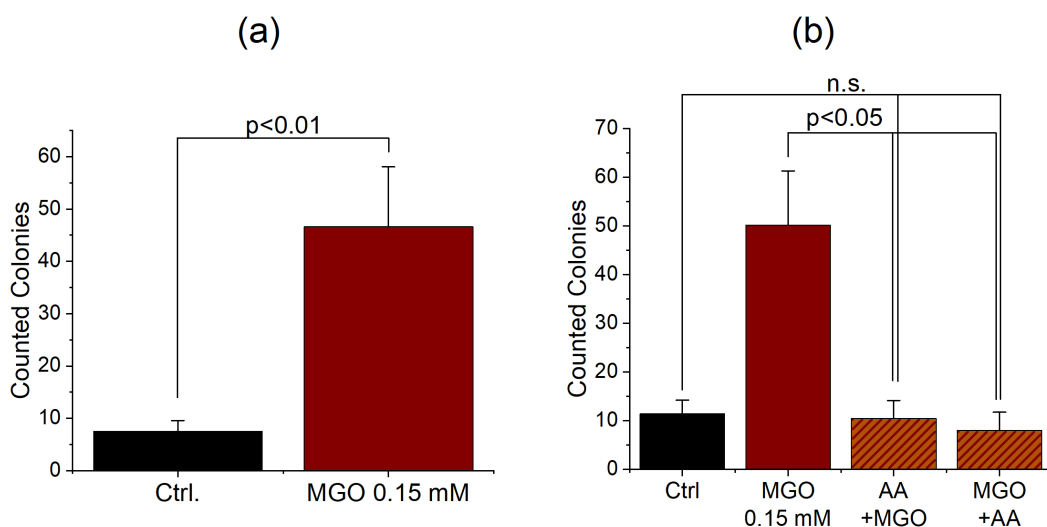


Figure 3. Increased microbial traversal through a BBB model upon treatment with MGO (a). THBMECs were treated with 0.15 mM MGO for 1 h. 450 μ L of bacteria suspension (OD 0.5) were put into each upper chamber. Medium from the lower chamber was plated on agar plates after 6 h. Graphs show the mean + SEM of counted colonies, untreated cells serve as control, (n = 3). Microbial traversal in the presence of ascorbic acid decreased in MGO-treated cells (b). THBMECs were treated with 0.15 mM MGO for 1 h. Afterwards, ascorbic acid with a concentration of 0.1 mM was administered to the treated cells. Additionally, cells were first treated with ascorbic acid for 4 h and afterwards glycated with MGO 0.15 mM for 1 h. 450 μ L of *E. coli* suspension (OD 0.5) was put into each upper chamber. Medium from the lower

chamber was plated on agar plates after 6 h. Graphs show the mean + SEM of counted colonies, untreated cells served as control, (n = 3).

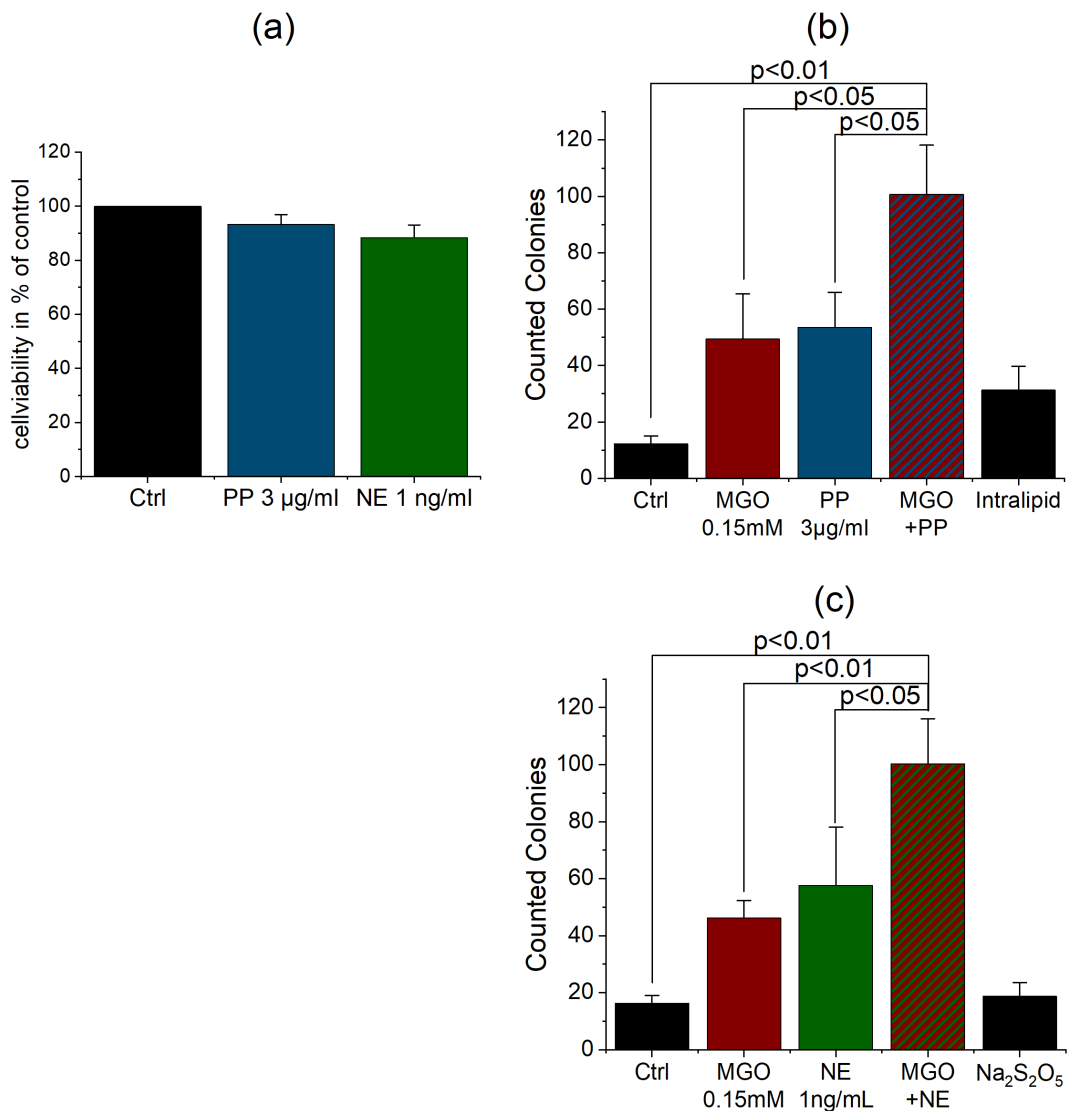


Figure 4. Cell viability of the compounds propofol (PP) and norepinephrine (NE) in endothelial cells (a). THBMECs were treated with 3 µg/mL propofol for 3 h and 1 ng/mL norepinephrine for 1 h. MTT assays were performed to analyze the cell viability after treatment. The graph shows the mean + SEM of the cell viability, untreated cells served as control, (n = 3). Microbial traversal in presence of propofol and norepinephrine with and without MGO treatment. THBMECs were treated with 0.15 mM MGO for 1 h. Afterwards, glycated and non-glycated cells were treated with 3 µg/mL propofol for 3 h (b) or with 1 ng/mL norepinephrine for 1 h (c). 450 µL of *E.coli* suspension (OD 0.5) were put into each upper chamber. Medium from the lower chamber was plated on agar plates after 6 h. The graph shows the mean + SEM of counted colonies, untreated cells and intralipid (b) or sodium metabisulfite (c) served as control, (n = 3).

3.4. Anesthetics Increase the Permeability of the BBB and Bacterial Traversal

Anesthetics are known to have an impact on permeability of the human blood-brain barrier. Therefore, we decided to test common anesthetics in the human BBB model. Additionally, we combined glycation and anesthetic treatment to exemplify replicate the situation of an older or diabetic person during surgery. We used propofol (PP) as one of the most common anesthetic compounds and norepinephrine (NE), which is used to compensate for a decrease of blood pressure caused by propofol. Treatment of cells was performed with 3 µg/mL propofol [37,38] and 1 ng/mL norepinephrine [39]. These concentrations are in the range of common blood levels during surgery. The propofol treatment lasted 3 h to simulate an average surgery. Norepinephrine is mostly used as bolus injection, so we treated cells for 1 h in our model.

Again, we performed cell viability assays for the treatment of cells with propofol 3 µg/mL for 3 h and norepinephrine 1 ng/mL for 1 h. The assay showed no toxic effect of propofol or norepinephrine treatment on THBMECs or interference with proliferation (Figure 4). Untreated cells served as control in this assay. According to the test results, we treated the THBMECs in our model after 14 d cultivation with 3 µg/mL propofol for 3 h or 1 ng/mL norepinephrine for 1 h. To see effects of AGE formation during surgery, we glycated cells first with 0.15 mM MGO for 1 h and treated them with propofol or norepinephrine. After treatment, the bacteria solution was put into the upper chamber and after 6 h, medium from the lower chamber was plated and colonies were counted. Untreated cells served as control. There was a significant increase of microbial traversal between non-glycated and glycated cells treated with propofol. As control, we used a soya oil solution (Intralipid), since common propofol compounds are mixed with soya oil. Additionally, we were able to show an increase of microbial traversal between non-glycated and glycated cells after norepinephrine treatment. Sodium metabisulfite served as control, because it is used for the preservation of norepinephrine.

4. Discussion

Our results demonstrated the effect of glycation on the permeability of the human blood-brain barrier. As many studies proved a correlation of diabetes with meningitis [19–21] and post-operative delirium (POD) [40], we were able to show an effect of AGE on our model of the human BBB. A significant increase of microbial traversal in the model of the BBB in THBMECs was observed after glycation with MGO. We used a low amount of MGO which did not affect the cell viability as MTT assays

(Figure 2d) indicate. This concentration is at the lower range of measured human serum concentrations of MGO (190 +/- 68 nmol/L) [35]. These results indicate an effect of AGE formation on the transcellular and intracellular barrier function of THBMECs, which is associated with paracellular or transcellular traversal of bacteria [22–24]. Furthermore, we measured the transendothelial electrical resistance (TEER) (Supplementary Figure S1) proving that a breakdown of the BBB is not causative for the resulting effects. A decrease of resistance after treatment with MGO, propofol, or norepinephrine could not be measured in our model.

The treatment with propofol and norepinephrine was performed with amounts as similar as possible to plasma concentrations during surgery [37–39]. To show effects in diabetic patients, cells were glycated with MGO before inoculating with bacteria. The single treatment with propofol indicates a damaging effect and a support of the breakdown of BBB as some studies also proposed [29,30]. As the effects of propofol are distinct in our experiments, we cannot confirm neuroprotective effects of propofol as some studies comparing to sevoflurane anesthesia propose [32]. Single treatment with norepinephrine increases the permeability of BBB as well. In animal models, high levels of norepinephrine correlated with POD [41], whereas the circumstances in humans have not been entirely elucidated so far [42]. Whilst norepinephrine is important for maintaining hemodynamical stability in ICU patients, it led to an increase of the microbial traversal across the BBB in THBMECs. The results indicate an additive effect of AGE formation and propofol or norepinephrine on the permeability of human blood-brain barrier (Figure 4). The wide influence of AGE on proteins and the effect of RAGE seem to amplify the negative effect of anesthesia on the permeability of human BBB. As diabetes is associated with a high level of AGE, the results highlight the importance of spare anesthesia in diabetic patients and a well-adjusted blood glucose level before surgery [43].

Since ascorbic acid is a reducing agent [44], it is able to prevent glycation of proteins like hemoglobin [45]. Our results demonstrate that ascorbic acid partly reverses the effect of glycation on the permeability of the human BBB (Figure 3b). Patients after surgery tend to have a high amount of reactive oxygen species (ROS), which often exceed their antioxidant capacity [46]. This leads to damage of macromolecules and ends up in organ dysfunction including POD. Ascorbic acid is known to be one of the most important antioxidants to reduce the influence of free radicals [47] and systemic inflammatory reaction [48]. In addition to the systemic impact of ascorbic acid, our experiments show a positive effect on glycated cells. As

hyperglycemia is associated with a high level of ROS [49], ascorbic acid prevents the formation of AGE [50]. Thus, our results indicate an effect of ascorbic acid after the formation of AGE. The human body depends on an adequate intake of vitamin C, as it is unable to synthesize ascorbic acid by itself. Given that 0.1 mM ascorbic acid has been used in the experiments, it reflects a realistic concentration, if 100 mg ascorbic acid are ingested in a person with a blood volume of 4–6 L on average. We propose that high levels of ascorbic acid in the body fluids may have beneficial effects of diabetic encephalopathy, which is accepted to be a major complication of diabetes mellitus and prevent adverse effects during anesthesia.

This model provides the possibility to test the influence of agents on the permeability of the human BBB, whereby the absolute measurement of bacteria traversal across the cell monolayer allows a fast testing to analyze further drugs.

Further research is needed to determine the mainly affected proteins. A screen via mass spectrometry could give first insights of altered protein levels and associated pathways, which could be confirmed with cell biological experiments. The route of the bacteria during the traversal from the apical side to the basolateral side is also not entirely clear. Thus, tracking experiments and monitoring of the bacteria by microscopy could help to elucidate their routes.

5. Conclusions

In summary, we could demonstrate an increase of microbial traversal across the human BBB after treatment with AGE as well as propofol and norepinephrine in our THBMEC model. Importantly, these results could be partially reversed upon the administration of ascorbic acid, which could have beneficial effects, if given prior to anesthesia.

Supplementary Materials: The following are available online at <http://www.mdpi.com/2077-0383/9/11/3672/s1>

(a)

CBU range 4.5 to 5.5	
CBU/mL	9,60357E+06

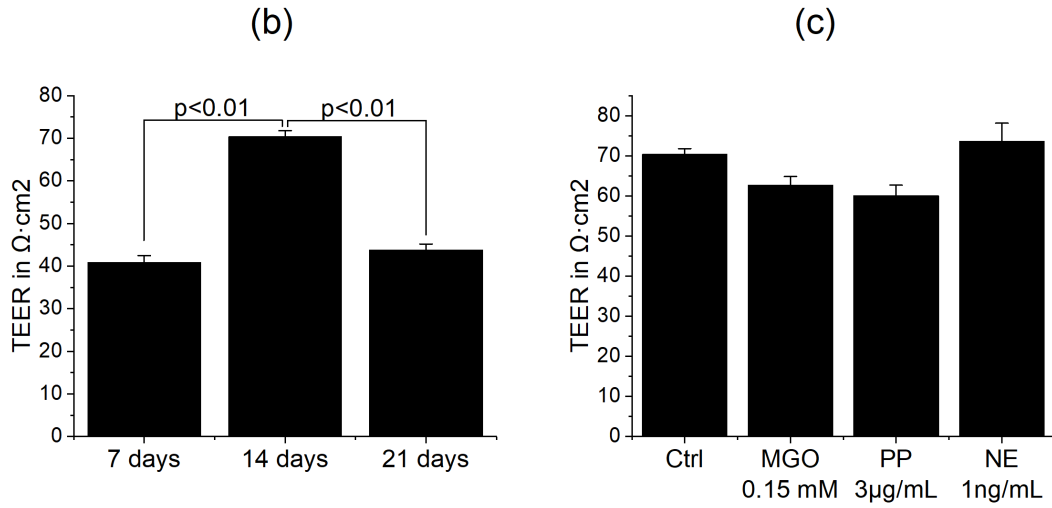


Figure S1: Measurement of Colony Building Units (CBU) at an optical density with a range from 4.5 to 5.5. at 570 nm (a). Transendothelial electrical resistance measured in the BBB model of THBMEC after different time points and treatments (b, c).

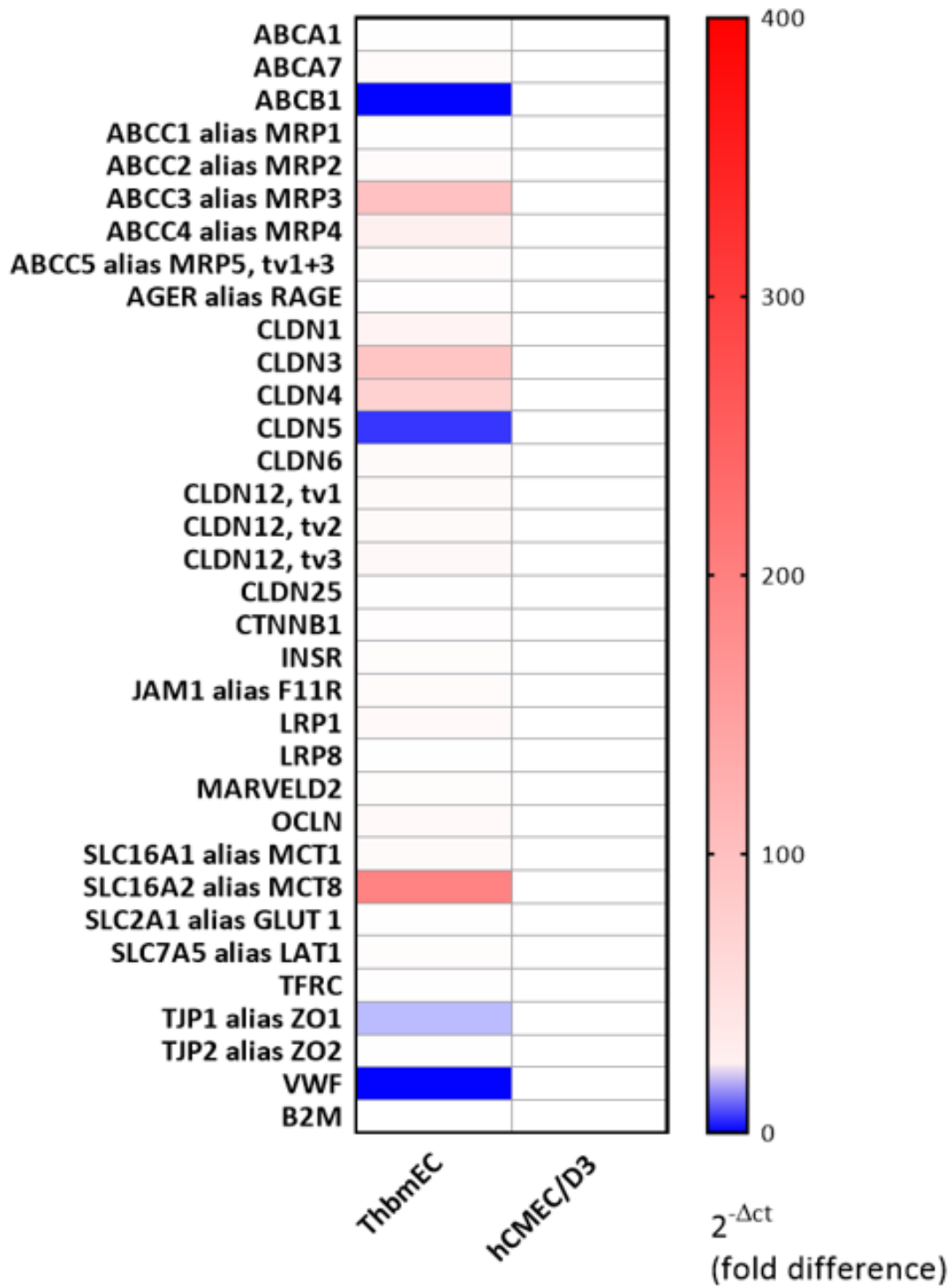


Figure S2: Heat map analysis of high-throughput multiplex barrier qPCR data of THBMEC cells in comparison to hCMEC/D3 cells as positive control, set to 1.0. Total RNA extracts were pre-amplified and the Ct values of the targets were normalized to the endogenous control B2M after qPCR.

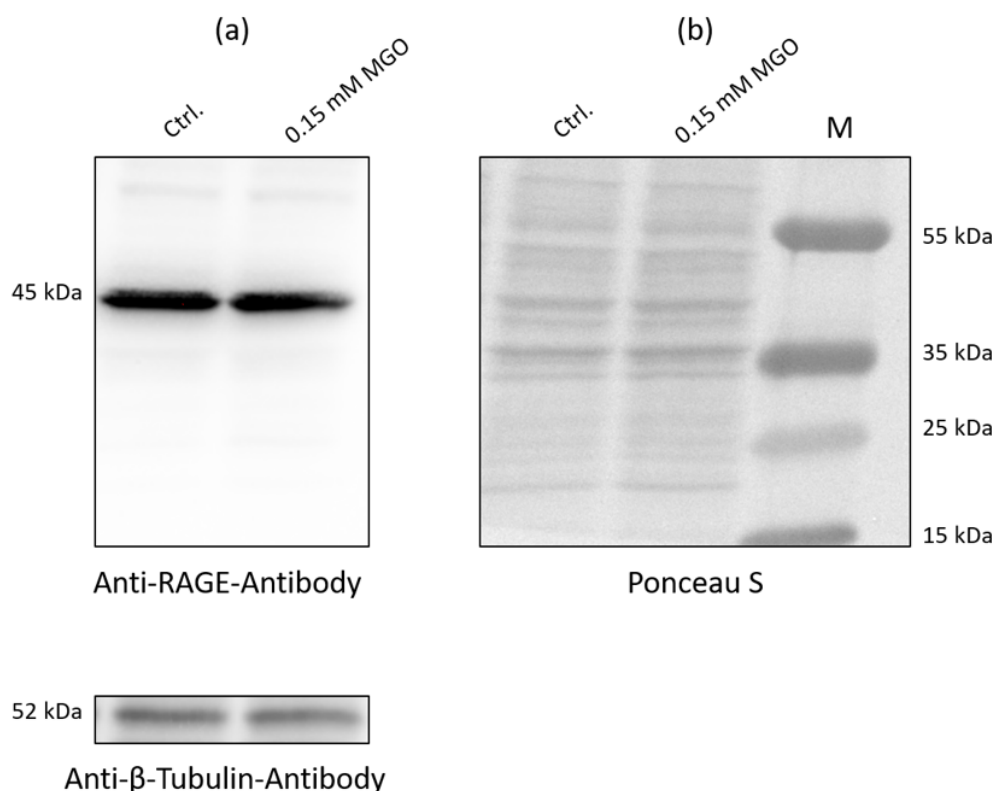


Figure S3: Expression levels of RAGE in THBMECs with or without MGO treatment. THBMECs were incubated with 0.15 mM MGO for 1 h in serum-free medium. Total protein was separated using SDS-PAGE. Expression of RAGE was detected by immuno-blotting using anti-RAGE-antibody (ab3611) (a). Tubulin detected with an anti-tubulin antibody as well as Ponceau S staining served as loading control (b).

Author Contributions: Conceptualization, V.W., H.O., K.B., and R.H.; formal analysis, V.W., H.O., T.L., and C.H.; writing—original draft preparation, H.O. and V.W.; writing—review and editing, V.W., H.O., C.H., K.B., B.H., and R.H.; visualization, V.W.; supervision, M.J., R.H., H.O., and K.B.; project administration, R.H.; funding acquisition, R.H. and B.H. All authors have read and agreed to the published version of the manuscript.

Funding: V.W., H.O. and R.H. were supported by the Deutsche Forschungsgemeinschaft (DFG, Germany) (RTG 2155, ProMoAge). T.L. was supported by the Wilhelm Roux Program HaPKoM.

Acknowledgments: The authors acknowledge Annett Thate for technical assistance.

Conflicts of Interest: The authors declare no conflict of interest.

References

1. Schalkwijk, C.G.; Miyata, T. Early- and advanced non-enzymatic glycation in diabetic vascular complications: the search for therapeutics. *Amino Acids* 2012, 42, 1193–1204, doi:10.1007/s00726-010-0779-9.
2. Bennmann, D.; Horstkorte, R.; Hofmann, B.; Jacobs, K.; Navarrete-Santos, A.; Simm, A.; Bork, K.; Gnanapragassam, V.S. Advanced glycation endproducts interfere with adhesion and neurite outgrowth. *PLoS ONE* 2014, 9, e112115, doi:10.1371/journal.pone.0112115.
3. Gkogkolou, P.; Bohm, M. Advanced glycation end products: Key players in skin aging? *Dermatoendocrinol* 2012, 4, 259–270, doi:10.4161/derm.22028.
4. John, W.G.; Lamb, E.J. The Maillard or browning reaction in diabetes. *Eye* 1993, 7, 230–237, doi:10.1038/eye.1993.55.
5. Singh, R.; Barden, A.; Mori, T.; Beilin, L. Advanced glycation end-products: a review. *Diabetologia* 2001, 44, 129–146, doi:10.1007/s001250051591.
6. Kalapos, M.P. Methylglyoxal and glucose metabolism: a historical perspective and future avenues for research. *Drug Metabol. Drug Interact.* 2008, 23, 69–91, doi:10.1515/dmdi.2008.23.1-2.69.
7. Ahmed, N.; Battah, S.; Karachalias, N.; Babaei-Jadidi, R.; Horanyi, M.; Baroti, K.; Hollan, S.; Thornalley, P.J. Increased formation of methylglyoxal and protein glycation, oxidation and nitrosation in triosephosphate isomerase deficiency. *Biochim. Biophys. Acta* 2003, 1639, 121–132, doi:10.1016/j.bbadis.2003.08.002.
8. Vistoli, G.; De Maddis, D.; Cipak, A.; Zarkovic, N.; Carini, M.; Aldini, G. Advanced glycoxidation and lipoxidation end products (AGEs and ALEs): an overview of their mechanisms of formation. *Free Radic. Res.* 2013, 47, 3–27, doi:10.3109/10715762.2013.815348.
9. Meredith, M.E.; Qu, Z.C.; May, J.M. Ascorbate reverses high glucose- and RAGE-induced leak of the endothelial permeability barrier. *Biochem. Biophys. Res. Commun.* 2014, 445, 30–35, doi:10.1016/j.bbrc.2014.01.078.
10. Banks, W.A. From blood-brain barrier to blood-brain interface: new opportunities for CNS drug delivery. *Nat. Rev. Drug. Discov.* 2016, 15, 275–292, doi:10.1038/nrd.2015.21.
11. Brightman, M.W.; Reese, T.S. Junctions between intimately apposed cell membranes in the vertebrate brain. *J. Cell Biol.* 1969, 40, 648–677, doi:10.1083/jcb.40.3.648.
12. Morris, A.W.; Sharp, M.M.; Albargothy, N.J.; Fernandes, R.; Hawkes, C.A.; Verma, A.; Weller, R.O.; Carare, R.O. Vascular basement membranes as

pathways for the passage of fluid into and out of the brain. *Acta Neuropathol* 2016, 131, 725–736, doi:10.1007/s00401-016-1555-z.

13. Luissint, A.C.; Artus, C.; Glacial, F.; Ganeshamoorthy, K.; Couraud, P.O. Tight junctions at the blood brain barrier: physiological architecture and disease-associated dysregulation. *Fluids Barriers CNS* 2012, 9, 23, doi:10.1186/2045-8118-9-23.
14. Harris, E.S.; Nelson, W.J. VE-cadherin: at the front, center, and sides of endothelial cell organization and function. *Curr. Opin. Cell Biol.* 2010, 22, 651–658, doi:10.1016/j.ceb.2010.07.006.
15. Kim, K.S.; Wass, C.A.; Cross, A.S. Blood-brain barrier permeability during the development of experimental bacterial meningitis in the rat. *Exp. Neurol.* 1997, 145, 253–257, doi:10.1006/exnr.1997.6458.
16. Kratz, T.; Heinrich, M.; Schlauß, E.; Diefenbacher, A. Preventing postoperative delirium. *Dtsch. Arztebl. Int.* 2015, 112, 289–296, doi:10.3238/arztebl.2015.0289.
17. Margiotta, A.; Bianchetti, A.; Ranieri, P.; Trabucchi, M. Clinical characteristics and risk factors of delirium in demented and not demented elderly medical inpatients. *J. Nutr. Health Aging* 2006, 10, 535–539.
18. Smulter, N.; Lingehall, H.C.; Gustafson, Y.; Olofsson, B.; Engstrom, K.G. Delirium after cardiac surgery: incidence and risk factors. *Interact. Cardiovasc. Thorac. Surg.* 2013, 17, 790–796, doi:10.1093/icvts/ivt323.
19. van Veen, K.E.; Brouwer, M.C.; van der Ende, A.; van de Beek, D. Bacterial meningitis in diabetes patients: a population-based prospective study. *Sci. Rep.* 2016, 6, 36996, doi:10.1038/srep36996.
20. Kalra, S.; Zargar, A.H.; Jain, S.M.; Sethi, B.; Chowdhury, S.; Singh, A.K.; Thomas, N.; Unnikrishnan, A.G.; Thakkar, P.B.; Malve, H. Diabetes insipidus: The other diabetes. *Indian J. Endocrinol. Metab.* 2016, 20, 9–21, doi:10.4103/2230-8210.172273.
21. Schut, E.S.; Westendorp, W.F.; de Gans, J.; Kruyt, N.D.; Spanjaard, L.; Reitsma, J.B.; van de Beek, D. Hyperglycemia in bacterial meningitis: a prospective cohort study. *BMC Infect. Dis.* 2009, 9, 57, doi:10.1186/1471-2334-9-57.
22. Shimizu, F.; Sano, Y.; Tominaga, O.; Maeda, T.; Abe, M.A.; Kanda, T. Advanced glycation end-products disrupt the blood-brain barrier by stimulating the release of transforming growth factor-beta by pericytes and vascular endothelial growth factor and matrix metalloproteinase-2 by endothelial cells in vitro. *Neurobiol Aging* 2013, 34, 1902–1912, doi:10.1016/j.neurobiolaging.2013.01.012.

23. Hussain, M.; Bork, K.; Gnanapragassam, V.S.; Bennmann, D.; Jacobs, K.; Navarette-Santos, A.; Hofmann, B.; Simm, A.; Danker, K.; Horstkorte, R. Novel insights in the dysfunction of human blood-brain barrier after glycation. *Mech. Ageing Dev.* 2016, 155, 48–54, doi:10.1016/j.mad.2016.03.004.
24. Li, Q.; Liu, H.; Du, J.; Chen, B.; Li, Q.; Guo, X.; Huang, X.; Huang, Q. Advanced glycation end products induce moesin phosphorylation in murine brain endothelium. *Brain Res.* 2011, 1373, 1–10, doi:10.1016/j.brainres.2010.12.032.
25. Kim, K.S.; Itabashi, H.; Gemski, P.; Sadoff, J.; Warren, R.L.; Cross, A.S. The K1 capsule is the critical determinant in the development of *Escherichia coli* meningitis in the rat. *J. Clin. Invest.* 1992, 90, 897–905, doi:10.1172/jci115965.
26. Doran, K.S.; Fulde, M.; Gratz, N.; Kim, B.J.; Nau, R.; Prasadarao, N.; Schubert-Unkmeir, A.; Tuomanen, E.I.; Valentin-Weigand, P. Host-pathogen interactions in bacterial meningitis. *Acta Neuropathol.* 2016, 131, 185–209, doi:10.1007/s00401-015-1531-z.
27. Kim, K.S. Mechanisms of microbial traversal of the blood-brain barrier. *Nat. Rev. Microbiol.* 2008, 6, 625–634, doi:10.1038/nrmicro1952.
28. Liu, W.-T.; Lv, Y.-J.; Yang, R.-C.; Fu, J.-Y.; Liu, L.; Wang, H.; Cao, Q.; Tan, C.; Chen, H.-C.; Wang, X.-R. New insights into meningitic *Escherichia coli* infection of brain microvascular endothelial cells from quantitative proteomics analysis. *J. Neuroinflammation* 2018, 15, 291, doi:10.1186/s12974-018-1325-z.
29. Sharma, H.S.; Pontén, E.; Gordh, T.; Eriksson, P.; Fredriksson, A.; Sharma, A. Propofol promotes blood-brain barrier breakdown and heat shock protein (HSP 72 kd) activation in the developing mouse brain. *CNS Neurol. Disord. Drug Targets* 2014, 13, 1595–1603, doi:10.2174/1871527313666140806122906.
30. Doronzio, A.; Lanni, F.; Ayrian, E.; Zhang, Y.P.; Bilotta, F.; Rosa, G. Postoperative delirium after anesthesia with propofol, sevoflurane or desflurane: The Pinocchio trial. Interim analysis of safety and preliminary results: 7AP3-6. *Eur. J. Anaesthesiol.* 2013, 30, 108–109.
31. Ishii, K.; Akiyama, D.; Hara, K.; Makita, T.; Sumikawa, K. [Influence of general anesthetics on the incidence of postoperative delirium in the elderly]. *Masui* 2011, 60, 856–858.
32. Ishii, K.; Makita, T.; Yamashita, H.; Matsunaga, S.; Akiyama, D.; Toba, K.; Hara, K.; Sumikawa, K.; Hara, T. Total intravenous anesthesia with propofol is associated with a lower rate of postoperative delirium in comparison with sevoflurane anesthesia in elderly patients. *J. Clin. Anesth.* 2016, 33, 428–431, doi:10.1016/j.jclinane.2016.04.043.
33. Weber, V.; Bork, K.; Horstkorte, R.; Olzscha, H. Analyzing the Permeability of the Blood-Brain Barrier by Microbial Traversal through Microvascular Endothelial Cells. *J. Vis. Exp.* 2020, doi:10.3791/60692.

34. Stins, M.F.; Badger, J.; Sik Kim, K. Bacterial invasion and transcytosis in transfected human brain microvascular endothelial cells. *Microb. Pathog.* 2001, 30, 19–28, doi:10.1006/mpat.2000.0406.
35. Dhananjayan, K.; Irrgang, F.; Raju, R.; Harman, D.G.; Moran, C.; Srikanth, V.; Münch, G. Determination of glyoxal and methylglyoxal in serum by UHPLC coupled with fluorescence detection. *Anal Biochem.* 2019, 573, 51–66, doi:10.1016/j.ab.2019.02.014.
36. Scheffler, J.; Bork, K.; Bezold, V.; Rosenstock, P.; Gnanapragassam, V.S.; Horstkorte, R. Ascorbic acid leads to glycation and interferes with neurite outgrowth. *Exp. Gerontol.* 2019, 117, 25–30, doi:10.1016/j.exger.2018.08.005.
37. Wessén, A.; Persson, P.M.; Nilsson, A.; Hartvig, P. Concentration-effect relationships of propofol after total intravenous anesthesia. *Anesth. Analg.* 1993, 77, 1000–1007.
38. Takizawa, E.; Hiraoka, H.; Takizawa, D.; Goto, F. Changes in the effect of propofol in response to altered plasma protein binding during normothermic cardiopulmonary bypass. *BJA Br. J. Anaesth.* 2005, 96, 179–185, doi:10.1093/bja/aei293.
39. Minami, K.; Körner, M.M.; Vyska, K.; Kleesiek, K.; Knobl, H.; Körfer, R. Effects of pulsatile perfusion on plasma catecholamine levels and hemodynamics during and after cardiac operations with cardiopulmonary bypass. *J. Thorac. Cardiovasc. Surg.* 1990, 99, 82–91.
40. Smulter, N.; LingeHall, H.C.; Gustafson, Y.; Olofsson, B.; Engström, K.G. Delirium after cardiac surgery: incidence and risk factors†. *Interact. Cardiovasc. Thorac. Surg.* 2013, 17, 790–796, doi:10.1093/icvts/ivt323.
41. Bhardwaj, A.; Brannan, T.; Martinez-Tica, J.; Weinberger, J. Ischemia in the dorsal hippocampus is associated with acute extracellular release of dopamine and norepinephrine. *J. Neural. Transm. Gen. Sect.* 1990, 80, 195–201, doi:10.1007/bf01245121.
42. Yasuda, Y.; Nishikimi, M.; Nishida, K.; Takahashi, K.; Numaguchi, A.; Higashi, M.; Matsui, S.; Matsuda, N. Relationship Between Serum Norepinephrine Levels at ICU Admission and the Risk of ICU-Acquired Delirium: Secondary Analysis of the Melatonin Evaluation of Lowered Inflammation of ICU Trial. *Crit. Care Explor.* 2020, 2, e0082, doi:10.1097/cce.0000000000000082.
43. Windmann, V.; Spies, C.; Knaak, C.; Wollersheim, T.; Piper, S.; Vorderwülbecke, G.; Kurpanik, M.; Kuenz, S.; Lachmann, G. Intraoperative hyperglycemia increases the incidence of postoperative delirium. *Minerva Anesthesiol.* 2019, 85, doi:10.23736/S0375-9393.19.13748-0.
44. Rao, G.G.; Rao, V.N. Ascorbic acid as a reducing agent in quantitative analysis. *Fresenius Z. Anal. Chem.* 1955, 147, 338–347, doi:10.1007/BF00432902.

45. Krone, C.A.; Ely, J.T. Ascorbic acid, glycation, glycohemoglobin and aging. *Med. Hypotheses* 2004, 62, 275–279, doi:10.1016/s0306-9877(03)00313-x.
46. Roy, J.; Galano, J.M.; Durand, T.; Le Guennec, J.Y.; Lee, J.C. Physiological role of reactive oxygen species as promoters of natural defenses. *FASEB J.* 2017, 31, 3729–3745, doi:10.1096/fj.201700170R.
47. Frei, B.; England, L.; Ames, B.N. Ascorbate is an outstanding antioxidant in human blood plasma. *Proc. Natl. Acad. Sci. USA* 1989, 86, 6377–6381, doi:10.1073/pnas.86.16.6377.
48. Hill, A.; Wendt, S.; Benstoem, C.; Neubauer, C.; Meybohm, P.; Langlois, P.; Adhikari, N.K.; Heyland, D.K.; Stoppe, C. Vitamin C to Improve Organ Dysfunction in Cardiac Surgery Patients-Review and Pragmatic Approach. *Nutrients* 2018, 10, doi:10.3390/nu10080974.
49. Volpe, C.M.O.; Villar-Delfino, P.H.; dos Anjos, P.M.F.; Nogueira-Machado, J.A. Cellular death, reactive oxygen species (ROS) and diabetic complications. *Cell Death Dis.* 2018, 9, 119, doi:10.1038/s41419-017-0135-z.
50. Vinson, J.; Howard, T. Inhibition of protein glycation and advanced glycation end products by ascorbic acid and other vitamins and nutrients. *J. Nutr. Biochem.* 1996, 7, 659–663, doi:10.1016/S0955-2863(96)00128-3.

Publisher's Note: MDPI stays neutral with regard to jurisdictional claims in published maps and institutional affiliations.

© 2020 by the authors. Submitted for possible open access publication under the terms and conditions of the Creative Commons Attribution (CC BY) license (<http://creativecommons.org/licenses/by/4.0/>).

Erklärungen

(1) Ich erkläre, dass ich mich an keiner anderen Hochschule einem Promotionsverfahren unterzogen bzw. eine Promotion begonnen habe.

(2) Ich erkläre, die Angaben wahrheitsgemäß gemacht und die wissenschaftliche Arbeit an keiner anderen wissenschaftlichen Einrichtung zur Erlangung eines akademischen Grades eingereicht zu haben.

(3) Ich erkläre an Eides statt, dass ich die Arbeit selbstständig und ohne fremde Hilfe verfasst habe. Alle Regeln der guten wissenschaftlichen Praxis wurden eingehalten; es wurden keine anderen als die von mir angegebenen Quellen und Hilfsmittel benutzt und die den benutzten Werken wörtlich oder inhaltlich entnommenen Stellen als solche kenntlich gemacht.

Datum, Unterschrift